

DESY 98-017  
August 2006

## ADVANCED LATTICE QCD\*

Martin Lüscher

*Deutsches Elektronen-Synchrotron DESY  
Notkestrasse 85, D-22603 Hamburg, Germany  
E-mail: luscher@mail.desy.de*

---

\*Lectures given at the Les Houches Summer School “Probing the Standard Model of Particle Interactions”, July 28 – September 5, 1997

## Contents

1	Introduction	1
1.1	Lattice QCD	1
1.2	Continuum limit	2
1.3	Non-perturbative renormalization	2
1.4	Contents & aims of the lectures	2
2	Lattice effects and the continuum limit	3
2.1	Preliminaries	3
2.2	Lattice effects in perturbation theory	4
2.3	Non-perturbative test for lattice effects	5
2.4	Effective continuum theory	6
2.5	Scope of the effective continuum theory	8
2.6	Elimination of redundant terms	9
2.7	Concluding remarks	10
3	$O(a)$ improvement	10
3.1	$O(a)$ improved action	10
3.2	Improvement of local fields	12
3.3	Renormalization	13
3.4	Is $O(a)$ improvement effective?	14
3.5	Synthesis	15
4	Chiral symmetry in lattice QCD	16
4.1	Chiral Ward identities	16
4.2	PCAC relation	17
4.3	Integrated Ward identities	17
4.4	Euclidean proof of the Goldstone theorem	18
4.5	PCAC relation on the lattice	19
4.6	Chiral symmetry & renormalization	20
4.7	Concluding remarks	21
5	Non-perturbative improvement	22
5.1	Boundary conditions	22
5.2	Correlation functions in finite volume	23

5.3	How large are the chiral symmetry violations?	24
5.4	Tests of chiral symmetry at tree-level of perturbation theory	25
5.5	Computation of $c_{\text{sw}}$	26
5.6	Results and further developments	27
6	Non-perturbative renormalization	29
6.1	Example	30
6.2	Hadronic renormalization schemes	31
6.3	Meanfield improved perturbation theory	32
6.4	Intermediate renormalization	33
6.5	Recursive finite-size technique	34
7	QCD in finite volume and the femto-universe	35
7.1	Physical situation from large to small volumes	35
7.2	Asymptotic freedom and the limit $L \rightarrow 0$	36
7.3	Finite-volume renormalization schemes	37
8	Computation of the running coupling	38
8.1	Strategy	38
8.2	Hadronic scheme	39
8.3	Finite-volume scheme	40
8.4	Matching at low energies	41
8.5	Non-perturbative renormalization group	42
8.6	Computation of the $\Lambda$ parameter	45
8.7	Conversion to the $\overline{\text{MS}}$ scheme	47
9	Conclusions and outlook	47

## 1 Introduction

At first sight quantum chromodynamics (QCD) appears to be a relatively simple theory with extensive symmetry properties and only few parameters. To the novice it must come as a surprise that the whole range of strong interaction phenomena can be described by such a beautiful mathematical structure. Of course we do not know for sure whether this is really the case, but the accumulated evidence strongly suggests this to be so.

The masses of the light hadrons and many other properties of these particles are very precisely known from experiment. On the theoretical side, however, it is difficult to compute these quantities from first principles, because of the nonlinearities of the basic equations and because the coupling constant is not small at low energies. Precision tests of QCD in this regime have consequently been rare and are essentially limited to those aspects of the theory that are determined by the (approximate) chiral and flavour symmetries. It is evidently of great importance to overcome this deficit and to verify that the same lagrangian which describes the interactions between quarks and gluons at high energies also explains the spectrum of light hadrons and their properties.

### 1.1 Lattice QCD

To be able to address this problem one first of all needs a formulation of the theory which is mathematically well-defined at the non-perturbative level. Such a framework is obtained by introducing a space-time lattice and discretizing the fields and the action. The lattice cuts off the high frequencies and makes the theory completely finite. Eventually the continuum limit should be taken and one then encounters the usual ultra-violet divergencies which can be removed through the usual parameter and operator renormalizations. Lattice QCD may thus be regarded as a non-perturbative regularization of the theory with a momentum cutoff inversely proportional to the lattice spacing.

Today quantitative results in lattice QCD are almost exclusively obtained using numerical simulations. Such calculations proceed by choosing a finite lattice which is sufficiently small that the quark and gluon fields can be stored in the memory of a computer. Through a Monte Carlo algorithm one then generates a representative ensemble of fields for the Feynman path integral and extracts the physical quantities from ensemble averages. Apart from statistical errors this method yields exact results for the chosen lattice parameters and is hence suitable for non-perturbative studies of QCD.

One should however not conclude that the theory can be solved through numerical simulations alone. Without physical insight and ingenious computational

strategies it would be quite impossible to obtain accurate results that can be compared with experiment.

### *1.2 Continuum limit*

One of the most important and difficult issues in lattice QCD is the continuum limit. In practice the limit is taken by computing the quantities of interest for several values of the lattice spacing  $a$  and extrapolating the results to  $a = 0$ . An obvious problem is then that one cannot afford to perform numerical simulations at arbitrarily small lattice spacings. In hadron mass calculations, for example, current lattice spacings are usually not much smaller than 0.1 fm. This will remain so for quite some time, because the simulation programs slow down proportionally to  $a^5$  (or even a larger power of  $a$ ) if all other parameters are held fixed.

In view of these remarks, it is not totally obvious that the continuum limit can be reached in a reliable manner from the presently accessible range of lattice spacings. A detailed theoretical understanding of the approach to the limit is certainly required for this and extensive numerical studies are then needed to confirm (or disprove) the expected behaviour.

### *1.3 Non-perturbative renormalization*

Non-perturbative renormalization is another topic where one would not get very far without theoretical input. Traditionally renormalization is discussed in the framework of perturbation theory, but when one is dealing with the low-energy sector of QCD the renormalization constants should be computed non-perturbatively. In more physical terms, the question is how precisely the perturbative regime of the theory is connected with the hadrons and their interactions. Evidently this is a fundamental aspect of QCD and not particularly a lattice issue.

Non-perturbative renormalization involves large scale differences and is hence not easily approached using numerical simulations, where the range of physical distances covered by any single lattice is rather limited. The problem has attracted a lot of attention recently and various ways to solve it have been proposed.

### *1.4 Contents & aims of the lectures*

The continuum limit and non-perturbative renormalization are the main themes of the lectures. In both areas significant progress has been made in the past few years. Chiral symmetry plays an important rôle in some of these developments and the way in which this symmetry is realized on the lattice is hence also discussed.

Another item which is given considerable weight are finite-size techniques. Such methods are probably unavoidable if one would like to overcome the limitations

imposed by the currently accessible lattices. Some of them have already proved to be very powerful and the aim of the lectures partly is to illustrate this and to provide a better understanding of the underlying physical picture.

The lectures are self-contained, but some familiarity with the basic concepts in lattice gauge theory is assumed throughout. It goes without saying that many interesting theoretical developments in lattice QCD are not covered and that the selected topics merely reflect the knowledge and preferences of the lecturer.

### *Acknowledgements*

I would like to thank the organizers of the school, particularly Rajan Gupta, for the opportunity to give these lectures and for some very pleasant and stimulating weeks at Les Houches. Much of the material presented here is based on work done by the ALPHA collaboration. I wish to thank the members of the collaboration for their long-term commitment and an enjoyable team-work.

## **2 Lattice effects and the continuum limit**

Nearly 20 years ago Symanzik set out to study the nature of the continuum limit in perturbation theory [1]. He showed that lattice theories can be described through an effective continuum theory in which the lattice spacing dependence is made explicit. This work later led him to propose a method to accelerate the approach to the continuum limit, which is now known as the Symanzik improvement programme [2,3]. In this section we discuss the effective continuum theory for lattice QCD. A particular form of improvement will be considered in section 3.

### *2.1 Preliminaries*

In the standard formulation of lattice QCD (which goes back to Wilson's famous paper of 1974 [4]) the quark fields  $\psi(x)$  reside on the sites  $x$  of the lattice and carry colour, flavour and Dirac indices as in the continuum theory. The gauge field is represented through a field of  $SU(3)$  matrices  $U(x, \mu)$  where  $\mu = 0, \dots, 3$  labels the space-time directions. None of these is special since we are in euclidean space, but  $\mu = 0$  is conventionally associated with the time direction.

Under a gauge transformation  $\Lambda(x)$  the fields transform according to

$$\psi(x) \rightarrow \Lambda(x)\psi(x), \quad U(x, \mu) \rightarrow \Lambda(x)U(x, \mu)\Lambda(x + a\hat{\mu})^{-1},$$

where  $\hat{\mu}$  denotes the unit vector in direction  $\mu$ . The forward difference operator

$$\nabla_{\mu}\psi(x) = \frac{1}{a}[U(x, \mu)\psi(x + a\hat{\mu}) - \psi(x)]$$

is hence gauge covariant. In the same way a backward difference operator  $\nabla_{\mu}^*$  may be defined and the lattice Dirac operator is then given by

$$D = \frac{1}{2} \{ \gamma_{\mu}(\nabla_{\mu}^* + \nabla_{\mu}) - a\nabla_{\mu}^* \nabla_{\mu} \}. \quad (1)$$

The second term (which is referred to as the Wilson term) is included to avoid the well-known “doubler” problem. It assigns a mass proportional to  $1/a$  to all modes with momenta of this order while the low-momentum modes are affected by corrections vanishing proportionally to  $a$ . In particular, only these modes survive in the continuum limit.

The QCD action on the lattice may now be written in the form

$$S = \frac{1}{g_0^2} \sum_p \text{tr} \{ 1 - U(p) \} + a^4 \sum_x \bar{\psi}(x)(D + m_0)\psi(x) \quad (2)$$

with  $g_0$  being the bare gauge coupling and  $m_0$  the bare quark mass. For simplicity we shall assume that the quark mass is the same for all flavours. The sum in the gauge field part of the action runs over all oriented plaquettes  $p$  and  $U(p)$  denotes the product of the gauge field variables around  $p$ .

EXERCISE: List all continuous and discrete symmetries of the lattice action and write down the corresponding transformations of the fields

## 2.2 Lattice effects in perturbation theory

In lattice QCD one is primarily interested in the non-perturbative aspects of the theory. Perturbation theory can, however, give important structural insights and it has proved useful to study the approach to the continuum limit in this framework. A remarkable result in this connection is that the existence of the limit has been rigorously established to all orders of the expansion [5,6].

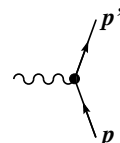
The Feynman rules on the lattice are derived straightforwardly from the lattice action by introducing the gluon field  $A_{\mu}(x)$  through

$$U(x, \mu) = \exp \{ g_0 a A_{\mu}(x) \}, \quad A_{\mu}(x) = A_{\mu}^a(x) \lambda^a,$$

and expanding in powers of  $g_0$ . One also needs to fix the gauge but this will not be discussed here (details can be found in ref. [6] for example). Compared to the

usual Feynman rules, an important difference is that the propagators and vertices are relatively complicated functions of the momenta and of the lattice spacing  $a$ . In particular, at tree-level all the lattice spacing dependence arises in this way.

A simple example illustrating this is the quark-gluon vertex



$$= -g_0 \lambda^a \left\{ \gamma_\mu - \frac{i}{2} a (p + p')_\mu + \mathcal{O}(a^2) \right\}. \quad (3)$$

It is immediately clear from this expression that the leading lattice corrections to the continuum term can be quite large even if the quark momenta  $p$  and  $p'$  are well below the momentum cutoff  $\pi/a$ . Moreover the corrections violate chiral symmetry, a fact that has long been a source of concern since many properties of low-energy QCD depend on this symmetry.

Lattice Feynman diagrams with  $l$  loops and engineering dimension  $\omega$  can be expanded in an asymptotic series of the form [1,2]

$$a^{-\omega} \sum_{k=0}^{\infty} \sum_{j=0}^l c_{kj} a^k [\ln(a)]^j.$$

After renormalization the negative powers in the lattice spacing and the logarithmically divergent terms cancel in the sum of all diagrams. The leading lattice corrections thus vanish proportionally to  $a$  (up to logarithms) at any order of perturbation theory.

EXERCISE: Work out the exact expression for the quark-gluon vertex and verify eq. (3)

### 2.3 Non-perturbative test for lattice effects

Sizeable lattice effects are also observed at the non-perturbative level when calculating hadron masses, for example. An impressive demonstration of this is obtained as follows. Let us suppose that the quark mass is adjusted so that the mass of the pseudo-scalar mesons coincides with the physical kaon mass. This sets the quark mass to about half the strange quark mass and one thus expects that the mass of the lightest vector meson is given by

$$m_V \simeq m_{K^*} = 892 \text{ MeV}.$$

Computations of the meson masses using numerical simulations however show that this is not the case at the accessible lattice spacings (see fig. 1). Instead one observes



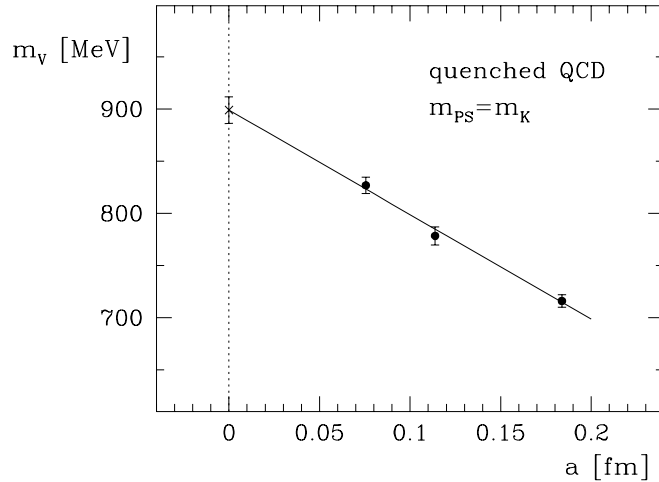


Figure 1: Calculated values of the vector meson mass (full circles) and linear extrapolation to the continuum limit (cross). Simulation data from Butler et al. (GF11 collab.) [7].

a strong dependence on the lattice spacing and it is only after extrapolating the data to  $a = 0$  that one ends up with a value close to expectations.

The numerical simulations quoted here have been performed in “quenched QCD” where sea quark effects are neglected. It seems unlikely, however, that a very different result would be obtained in the full theory. Perturbation theory and the calculations in quenched QCD rather suggest that large lattice effects already arise from the interaction between the gluon field and the valence quarks and these are not suppressed when the sea quarks are included.

#### 2.4 *Effective continuum theory*

In phenomenology it is well-known that the effects of as yet undetected substructures or heavy particles may be described by adding higher-dimensional interaction terms to the Standard Model lagrangian. From the point of view of an underlying more complete theory, the Standard Model together with the added terms is then a low-energy effective theory.

A similar situation occurs in lattice QCD, where the momentum cutoff may be regarded (in a purely mathematical sense) as a scale of new physics. The associated

low-energy effective theory is a continuum theory with action [2,3]

$$S_{\text{eff}} = \int d^4x \left\{ \mathcal{L}_0(x) + a\mathcal{L}_1(x) + a^2\mathcal{L}_2(x) + \dots \right\}, \quad (4)$$

where  $\mathcal{L}_0$  denotes the continuum QCD lagrangian and the  $\mathcal{L}_k$ 's,  $k \geq 1$ , are linear combinations of local operators of dimension  $4 + k$ . The dimension counting here includes the (non-negative) powers of the quark mass  $m$  by which some of the fields may be multiplied. From the list of all possible such fields only those need to be considered which are invariant under the symmetries of the lattice theory. Many terms can also be eliminated using partial integration.

In the following we shall be mainly interested in the lattice corrections of order  $a$ . All other corrections are proportional to higher powers of  $a$  and are thus expected to be less important at small lattice spacings. Taking the symmetries of the lattice action into account, it is not difficult to show that the effective lagrangian  $\mathcal{L}_1$  may be written as a linear combination of the fields

$$\begin{aligned} \mathcal{O}_1 &= \bar{\psi} i\sigma_{\mu\nu} F_{\mu\nu} \psi, \\ \mathcal{O}_2 &= \bar{\psi} D_\mu D_\mu \psi + \bar{\psi} \overleftarrow{D}_\mu \overleftarrow{D}_\mu \psi, \\ \mathcal{O}_3 &= m \text{tr} \{ F_{\mu\nu} F_{\mu\nu} \}, \\ \mathcal{O}_4 &= m \left\{ \bar{\psi} \gamma_\mu D_\mu \psi - \bar{\psi} \overleftarrow{D}_\mu \gamma_\mu \psi \right\}, \\ \mathcal{O}_5 &= m^2 \bar{\psi} \psi, \end{aligned}$$

where  $F_{\mu\nu}$  denotes the gauge field strength and  $D_\mu$  the gauge covariant partial derivative.

In the effective continuum theory, renormalized lattice fields are represented through effective fields of the form

$$\phi_{\text{eff}} = \phi_0 + a\phi_1 + a^2\phi_2 + \dots \quad (5)$$

The fields  $\phi_0, \phi_1, \dots$  which can occur here must have the appropriate dimension and transform under the lattice symmetries in the same way as the lattice field which is being represented. As an example let us consider the isovector axial current

$$A_\mu^a(x) = \bar{\psi}(x) \gamma_\mu \gamma_5 \frac{1}{2} \tau^a \psi(x). \quad (6)$$

In this case the leading correction  $\phi_1$  can be shown to be a linear combination of the fields

$$(\mathcal{O}_6)_\mu^a = \bar{\psi} \gamma_5 \frac{1}{2} \tau^a \sigma_{\mu\nu} D_\nu \psi - \bar{\psi} \overleftarrow{D}_\nu \sigma_{\mu\nu} \gamma_5 \frac{1}{2} \tau^a \psi,$$

$$\begin{aligned}
(\mathcal{O}_7)_\mu^a &= \partial_\mu \left\{ \bar{\psi} \gamma_5 \frac{1}{2} \tau^a \psi \right\}, \\
(\mathcal{O}_8)_\mu^a &= m \bar{\psi} \gamma_\mu \gamma_5 \frac{1}{2} \tau^a \psi.
\end{aligned}$$

For other low-dimensional fields, such as the vector currents and the scalar and pseudo-scalar densities, the general form of the  $\mathcal{O}(a)$  corrections is also easily found. The number of terms is however rapidly increasing when one considers operators involving four quark fields or higher derivatives.

EXERCISE: Prove that any local field of dimension 5 respecting the symmetries of the lattice theory can be written as a linear combination of the basis  $\mathcal{O}_1, \dots, \mathcal{O}_5$  up to derivative terms

### 2.5 Scope of the effective continuum theory

So far we did not specify how precisely the lattice theory is related to the effective continuum theory. One must be a bit careful here, because additional lattice effects can arise when integrating correlation functions over short-distance regions. Such effects are characteristic of the correlation functions considered and are not accounted for by the effective action and the effective fields. In the following attention will thus be restricted to position space correlation functions at non-zero (physical) distances. This restriction is not very severe, since most physical quantities, including the hadron masses and matrix elements of local operators between particle states, can be extracted from such correlation functions.

So let us consider some local gauge invariant field  $\phi(x)$  constructed from the quark and gauge fields on the lattice. For simplicity we assume that  $\phi(x)$  does not mix with other fields under renormalization. We then expect that the connected renormalized  $n$ -point correlation functions

$$G_n(x_1, \dots, x_n) = (Z_\phi)^n \langle \phi(x_1) \dots \phi(x_n) \rangle_{\text{con}}$$

have a well-defined continuum limit, provided the renormalization factor  $Z_\phi$  is chosen appropriately and if all points  $x_1, \dots, x_n$  are kept at non-zero distances from one another.

In the effective continuum theory, the lattice correlation functions are represented through an asymptotic expansion

$$\begin{aligned}
G_n(x_1, \dots, x_n) &= \langle \phi_0(x_1) \dots \phi_0(x_n) \rangle_{\text{con}} \\
&\quad - a \int d^4y \langle \phi_0(x_1) \dots \phi_0(x_n) \mathcal{L}_1(y) \rangle_{\text{con}}
\end{aligned}$$

$$+a \sum_{k=1}^n \langle \phi_0(x_1) \dots \phi_1(x_k) \dots \phi_0(x_n) \rangle_{\text{con}} + \mathcal{O}(a^2), \quad (7)$$

where the expectation values on the right-hand side are to be taken in the continuum theory with lagrangian  $\mathcal{L}_0$ . The second term is the contribution of the  $\mathcal{O}(a)$  correction in the effective action. Note that the integral over  $y$  in general diverges at the points  $y = x_k$ . A subtraction prescription must hence be supplied. The precise way in which this happens is unimportant, because the arbitrariness that one has amounts to a local operator insertion at these points, i.e. to a redefinition of the field  $\phi_1(x)$ .

It should be emphasized at this point that not all the dependence on the lattice spacing comes from the explicit factors of  $a$  in eq. (7). The other source of  $a$ -dependence are the operators  $\phi_1$  and  $\mathcal{L}_k$ , which are linear combinations of some basis of fields. While the basis elements are independent of  $a$ , the coefficients need not be so, although they are expected to vary only slowly with  $a$ . In perturbation theory the coefficients are calculable polynomials in  $\ln(a)$ .

## 2.6 Elimination of redundant terms

The list of operators given above for the  $\mathcal{O}(a)$  lattice corrections can be reduced using the field equations. Formal application of the field equations yields the relations

$$\mathcal{O}_1 - \mathcal{O}_2 + 2\mathcal{O}_5 = 0, \quad \mathcal{O}_4 + 2\mathcal{O}_5 = 0, \quad (8)$$

which allow one to eliminate  $\mathcal{O}_2$  and  $\mathcal{O}_4$ , for example.  $\mathcal{O}_6$  is also redundant since it can be expressed as a linear combination of  $\mathcal{O}_7$  and  $\mathcal{O}_8$ .

There are two technical remarks which should be made here. The first is that in euclidean correlation functions the field equations are only valid up to contact terms. In eq. (7) these can arise when  $y$  gets close to one of the points  $x_k$ . The possible contact terms there however amount to an operator insertion, which can be compensated by a redefinition of  $\phi_1$ . The latter thus depends on exactly which basis of operators has been selected for the  $\mathcal{O}(a)$  effective action. Note that when the field equations are used to simplify  $\phi_1$ , no contact terms can arise since all points  $x_k$  keep away from each other.

The second observation is that renormalization and operator mixing must be taken into account when deriving operator relations from the field equations. In particular, the naive relations, eq. (8), are only valid at tree-level of perturbation theory. At higher orders they are replaced by linear combinations of all basis elements with coefficients that depend on the coupling and the chosen normalization conditions. Barring singular events, it is then still possible to eliminate  $\mathcal{O}_2$ ,  $\mathcal{O}_4$  and  $\mathcal{O}_6$ .

EXERCISE: Work out the free quark propagator on the lattice and check that its dependence on the lattice spacing matches with what is expected from the effective theory

### 2.7 Concluding remarks

Through the effective continuum theory a better understanding of the approach to the continuum limit is achieved. In particular, omitting terms that are redundant or which amount to renormalizations of the coupling and the quark mass, the leading lattice correction in the effective action is proportional to the Pauli term  $\bar{\psi} i\sigma_{\mu\nu} F_{\mu\nu} \psi$ . The lattice thus assigns an anomalous colour-magnetic moment of order  $a$  to the quarks. Very many more terms contribute to  $\mathcal{L}_2$  and a simple physical interpretation is not easily given. The pattern of the lattice effects of order  $a^2$  should hence be expected to be rather complicated.

## 3 $O(a)$ improvement

While the general form of the effective continuum theory is determined by the field content and the symmetries of the lattice theory, the coefficients multiplying the basis fields in the effective action and the effective fields depend on how precisely the latter has been set up. With an improved lattice action and improved expressions for the local composite fields we may hence be able to reduce the size of the lattice effects and thus to accelerate the convergence to the continuum limit [2,3]. The idea is similar to using higher-order discretization schemes for the numerical solution of partial differential equations, but the situation is not quite as simple because of the non-linearities and the associated renormalization effects.

Improvement can be implemented in different ways and there is currently no single preferred way to proceed. The subject has been reviewed by Niedermayer [8] and many interesting contributions have been made since then.  $O(a)$  improvement is a relatively modest approach, where one attempts to cancel all lattice effects of order  $a$ . This development started a long time ago [9–13] and the method is now becoming increasingly usable although there are still a few loose ends.

### 3.1 $O(a)$ improved action

In the following our aim is to construct an improved lattice action by adding a suitable counterterm to the Wilson action eq. (2). The counterterm should be chosen such that the order  $a$  term in the action of the effective continuum theory is cancelled. We are only interested in position space correlation functions of the type discussed

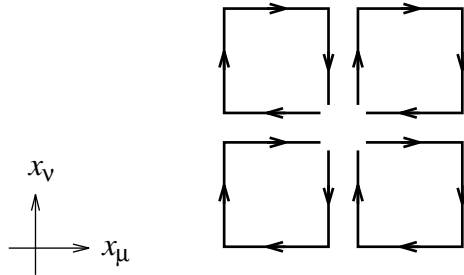


Figure 2: Graphical representation of the products of gauge field variables contributing to the lattice field tensor [eq. (10)]. The point  $x$  is at the centre of the diagram where all loops start and end.

above and may hence assume that the effective lagrangian  $\mathcal{L}_1$  is a linear combination of the reduced basis of fields  $\mathcal{O}_1$ ,  $\mathcal{O}_3$  and  $\mathcal{O}_5$ . It is then quite obvious that  $\mathcal{L}_1$  can be made to vanish by adding a counterterm of the form

$$\delta S = a^5 \sum_x \left\{ c_1 \widehat{\mathcal{O}}_1(x) + c_3 \widehat{\mathcal{O}}_3(x) + c_5 \widehat{\mathcal{O}}_5(x) \right\},$$

where  $\widehat{\mathcal{O}}_k$  is some lattice representation of the field  $\mathcal{O}_k$ .

Apart from renormalizations of the bare parameters and adjustments of the coefficients  $c_k$ , the discretization ambiguities that one has here are of order  $a^2$ . In particular, we may choose to represent the fields  $\text{tr}\{F_{\mu\nu}F_{\mu\nu}\}$  and  $\bar{\psi}\psi$  by the plaquette field and the local scalar density that already appear in the Wilson action. The terms proportional  $\widehat{\mathcal{O}}_3$  and  $\widehat{\mathcal{O}}_5$  then amount to a rescaling of the bare coupling and mass by factors of the form  $1 + \mathcal{O}(am)$ . We ignore this rescaling for the time being and return to the issue later when we discuss the renormalization of the improved theory.

For the improved action we thus obtain

$$S = S_{\text{Wilson}} + a^5 \sum_x c_{\text{sw}} \bar{\psi}(x) \frac{i}{4} \sigma_{\mu\nu} \widehat{F}_{\mu\nu}(x) \psi(x), \quad (9)$$

where  $\widehat{F}_{\mu\nu}$  is a lattice representation of the gluon field tensor. Recall that the product of the gauge field variables around a plaquette in the  $(\mu, \nu)$ -plane is equal to  $1 + a^2 F_{\mu\nu} + \dots$  in the classical continuum limit. A symmetric definition of the lattice field tensor is hence given by

$$\widehat{F}_{\mu\nu}(x) = \frac{1}{8a^2} \{Q_{\mu\nu}(x) - Q_{\nu\mu}(x)\} \quad (10)$$

with  $Q_{\mu\nu}(x)$  being the sum of the plaquette loops shown in fig. 2.

The improved action, eq. (9), first appeared in a paper by Sheikholeslami and Wohlert in 1985 [12]. It did not receive too much attention at the time, because systematic studies of lattice effects were not feasible with the available computers. The situation has now changed and there is general agreement that improvement is useful or even necessary, particularly in full QCD where simulations are exceedingly expensive in terms of computer time.

To achieve the desired improvement, the coefficient  $c_{\text{sw}}$  multiplying the  $O(a)$  counterterm in the improved action should be chosen appropriately. For various technical reasons this is a non-trivial task and the tuning of  $c_{\text{sw}}$  has long been considered a weak point of the method. Sheikholeslami and Wohlert calculated the coefficient at tree-level of perturbation theory and Wohlert [13] later obtained the one-loop formula

$$c_{\text{sw}} = 1 + 0.2659 \times g_0^2 + O(g_0^4). \quad (11)$$

More recently a strategy has been developed which allows one to compute  $c_{\text{sw}}$  non-perturbatively using numerical simulations [14]. Chiral symmetry plays an important rôle in this context and the further discussion of this issue is hence postponed to section 5.

EXERCISE: Write down the expression for the lattice field tensor explicitly and check that it transforms under the lattice symmetries in the expected way

### 3.2 Improvement of local fields

Through the improvement of the action one achieves that on-shell quantities such as particle masses and scattering matrix elements approach the continuum limit with a rate proportional to  $a^2$ . As can be seen from eq. (7), some terms of order  $a$  however remain uncanceled in correlation functions of local fields. For a complete improvement of such correlation functions one also needs to improve the fields and to specify appropriate renormalization conditions.

Improved fields are constructed by adding local counterterms to the unimproved fields in such a way that the order  $a$  term in the associated effective fields is cancelled. The counterterms are linear combinations of a basis of operators with the appropriate dimension and symmetry properties. In the case of the isovector axial current, for example, the basis consists of a lattice representation of the fields  $\mathcal{O}_6$ ,  $\mathcal{O}_7$  and  $\mathcal{O}_8$ . The first of these is redundant and may be dropped without loss. The term associated with  $\mathcal{O}_8$  amounts to a renormalization of the current and is hence only meaningful when a renormalization condition has been imposed. Since we have not done so at this point, we drop this term too and shall address the issue again in the next subsection.

We are then left with a single term and the improved axial current becomes

$$(A_I)_\mu^a = A_\mu^a + c_A a \tilde{\partial}_\mu P^a, \quad (12)$$

where  $\tilde{\partial}_\mu$  denotes the average of the forward and backward difference operators and

$$P^a(x) = \bar{\psi}(x) \gamma_5 \frac{1}{2} \tau^a \psi(x) \quad (13)$$

the isovector pseudo-scalar density. The coefficient  $c_A$  depends on  $g_0$  and should be chosen so as to achieve the  $O(a)$  improvement of the correlation functions of the axial current. In perturbation theory one obtains [15]

$$c_A = -0.00756 \times g_0^2 + O(g_0^4)$$

and in quenched QCD the coefficient is now also known non-perturbatively [16].

EXERCISE: Show that the pseudo-scalar density, eq. (13), is already improved, i.e. no  $O(a)$  counterterm is needed in this case

### 3.3 Renormalization

When deriving the improved action and the expression eq. (12) for the improved axial current, all terms that amount to renormalizations of the coupling constant, the quark mass and the current by factors of the form  $1 + O(am)$  have been dropped. The reason for this has been that such factors should better be discussed in the context of renormalization which we now do.

In QCD with only light quarks it is technically advantageous to employ so-called mass-independent renormalization schemes. If we ignore  $O(a)$  improvement for while, the renormalized coupling and quark mass in such schemes are related to the bare parameters through

$$\begin{aligned} g_R^2 &= g_0^2 Z_g(g_0^2, a\mu), \\ m_R &= m_q Z_m(g_0^2, a\mu), \quad m_q = m_0 - m_c. \end{aligned}$$

The important point here is that the renormalization factors only depend on the normalization mass  $\mu$  and the coupling, but not on the quark mass. Note that an additive quark mass renormalization  $m_c$  (equal to  $1/a$  times some function of  $g_0$ ) is required on the lattice, because chiral symmetry is not preserved.

In the improved theory the definition of the renormalized parameters must be slightly modified, as otherwise one may end up with uncancelled cutoff effects of



order  $am_q$  in some correlation functions. From our discussion above one infers that we should first rescale the bare parameters according to

$$\begin{aligned}\tilde{g}_0^2 &= g_0^2 (1 + b_g am_q), \\ \tilde{m}_q &= m_q (1 + b_m am_q),\end{aligned}$$

and then define the renormalized coupling and mass through

$$\begin{aligned}g_R^2 &= \tilde{g}_0^2 Z_g(\tilde{g}_0^2, a\mu), \\ m_R &= \tilde{m}_q Z_m(\tilde{g}_0^2, a\mu).\end{aligned}$$

The coefficients  $b_g$  and  $b_m$  depend on  $g_0$  and must be chosen appropriately to cancel any remaining lattice effects of order  $am_q$ . They have been worked out to one-loop order of perturbation theory [18,19] and  $b_m$  is now also known non-perturbatively in quenched QCD [20].

Factors of the form  $1 + O(am_q)$  must also be included in the definition of renormalized improved fields. The renormalized axial current, for example, is given by

$$(A_R)_\mu^a = Z_A (1 + b_A am_q) (A_I)_\mu^a$$

and similar formulae apply to any multiplicatively renormalizable field. Even though the renormalized fields are written in this way, it should be noted that the  $b$ -coefficients do not depend on the renormalization conditions which are being imposed. The latter should be set up at zero quark masses and only fix the  $Z$ -factors.

EXERCISE: Consider the free quark theory and prove that  $b_m = -\frac{1}{2}$  in this case. Determine the renormalization factor needed to improve the position space correlation functions of the quark field

### 3.4 Is $O(a)$ improvement effective?

Numerical studies of lattice QCD using the improved action eq. (9) have been initiated a few years ago [21–24]. The additional computational work required for the improvement term generally takes less than 20% of the total computer time spent for the simulations, also in the unquenched case [37]. An important question which one would like to answer with these studies is whether the lattice effects on the quantities of physical interest are indeed significantly reduced at the accessible lattice spacings. For the non-perturbatively determined values of  $c_{sw}$  several collaborations have recently set out to check this [25–30], but it is too early to draw definite conclusions.

For illustration let us again consider the calculation of the vector meson mass  $m_V$  discussed in subsection 2.3. A preliminary analysis of simulation results from the UKQCD collaboration gives, for the  $O(a)$  improved theory,  $m_V = 924(17)$  MeV at  $a = 0.098$  fm and  $m_V = 932(26)$  MeV at  $a = 0.072$  fm [27,29]. These numbers do not show any significant dependence on the lattice spacing and they are also compatible with the value  $m_V = 899(13)$  that one obtains through extrapolation to  $a = 0$  of the results from the unimproved theory (left-most point in fig. 1). Data at larger values of the lattice spacing recently published by Edwards et al. [30] corroborate these findings.

Other quantities that are being studied include the pseudo-scalar and vector meson decay constants and the renormalized quark masses. Compared to the hadron mass calculations, the situation in these cases is significantly more complicated, because one also needs to determine the appropriate renormalization factors and the improved expressions for the isovector axial and vector currents. The experience accumulated so far suggests that the residual lattice effects are indeed small if  $a \leq 0.1$  fm. Further confirmation is however still needed.

### 3.5 *Synthesis*

At sufficiently small lattice spacings the effective continuum theory provides an elegant description of the approach to the continuum limit. Whether the currently accessible lattice spacings are in the range where the effective theory applies is not immediately clear, but the observed pattern of the lattice spacing dependence in the unimproved theory and the fact that  $O(a)$  improvement appears to work out strongly indicate this to be so. Very much smaller lattice spacings are then not required to reliably reach the continuum limit. It is evidently of great importance to put this conclusion on firmer grounds by continuing and extending the ongoing studies of  $O(a)$  improvement and other forms of improvement.

## 4 Chiral symmetry in lattice QCD

Many properties of low-energy QCD can be explained through the flavour and chiral symmetries of the theory. For the analysis of the weak interactions of the quarks, these symmetries are also very important and the fact that chiral symmetry is not exactly preserved on the lattice thus is a source of concern. In this section we discuss how precisely the symmetry is violated and indicate how to make use of it even though it is only approximate.

### 4.1 Chiral Ward identities

We first consider the theory in the continuum limit and proceed formally, i.e. without paying attention to the proper definition of the correlation functions that occur. We assume that there is an isospin doublet of quarks with equal mass  $m$  and study the associated chiral transformations.

In euclidean space the expectation value of any product  $\mathcal{O}$  of local composite fields is given by the functional integral

$$\langle \mathcal{O} \rangle = \frac{1}{\mathcal{Z}} \int_{\text{fields}} \mathcal{O} e^{-S}.$$

Starting from this expression the general chiral Ward identity is obtained by applying an infinitesimal chiral rotation

$$\delta\psi(x) = \omega^a(x) \frac{1}{2} \tau^a \gamma_5 \psi(x), \quad \delta\bar{\psi}(x) = \omega^a(x) \bar{\psi}(x) \gamma_5 \frac{1}{2} \tau^a,$$

to the integration variables. In these equations  $\tau^a$  denotes a Pauli matrix acting on the isospin indices of the quark field and  $\omega^a(x)$  is a smooth function which vanishes outside some bounded region  $R$ . Since the Pauli matrices are traceless, it is obvious that the integration measure is invariant under the transformation and we thus conclude that

$$\langle \delta S \mathcal{O} \rangle = \langle \delta \mathcal{O} \rangle. \quad (14)$$

The chiral variation of the action and of the local fields of interest are easily worked out. In particular, for the variation of the action one finds

$$\delta S = \int d^4x \omega^a \left\{ -\partial_\mu A_\mu^a + 2mP^a \right\}, \quad (15)$$

where  $A_\mu^a$  and  $P^a$  denote the isovector axial current and density [eqs. (6),(13)]. The derivation of this result involves a partial integration and it has been important here that  $\omega^a(x)$  smoothly goes to zero outside some bounded domain as otherwise a boundary term might arise.

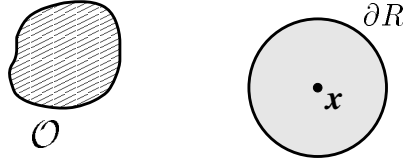


Figure 3: Choice of the region  $R$  when deriving the PCAC relation. The product of fields  $\mathcal{O}$  is assumed to be localized in the shaded area away from  $R$ .

By inserting particular products of fields  $\mathcal{O}$  and by choosing different functions  $\omega^a(x)$ , many useful relations (collectively referred to as the chiral Ward identities) are thus obtained. A few special cases will be considered in the following paragraphs.

EXERCISE: Show that the axial current  $A_\mu^a$  and the isovector vector current  $V_\mu^a = \bar{\psi}\gamma_\mu\frac{1}{2}\tau^a\psi$  transform into each other under infinitesimal chiral rotations

#### 4.2 PCAC relation

Let us first assume that the fields in the product  $\mathcal{O}$  are localized outside the region  $R$  as shown in fig. 3. The variation  $\delta\mathcal{O}$  vanishes under these conditions and eq. (14) reduces to  $\langle\delta S\mathcal{O}\rangle = 0$ . Since this equation holds for all functions  $\omega^a(x)$  with support in  $R$ , it follows that

$$\langle\partial_\mu A_\mu^a(x)\mathcal{O}\rangle = 2m\langle P^a(x)\mathcal{O}\rangle. \quad (16)$$

At zero quark mass this identity expresses the conservation of the axial current and it is hence referred to as the partially conserved axial current (PCAC) relation.

It should be emphasized that eq. (16) holds irrespectively of the product  $\mathcal{O}$  of fields as long as these are localized in a region not containing  $x$ . Of course this is just a reflection of the fact that the PCAC relation becomes an operator identity when the theory is set up in Minkowski space. Different choices of  $\mathcal{O}$  then correspond to considering different matrix elements of the operator relation.

EXERCISE: Derive the general Ward identity associated with the SU(2) flavour group. What happens if the quarks have unequal masses?

#### 4.3 Integrated Ward identities

Another class of identities is obtained when  $\mathcal{O}$  factors into two products of fields,  $\mathcal{O}_{\text{int}}$  and  $\mathcal{O}_{\text{ext}}$ , localized inside and outside the region  $R$  respectively (see fig. 4). In

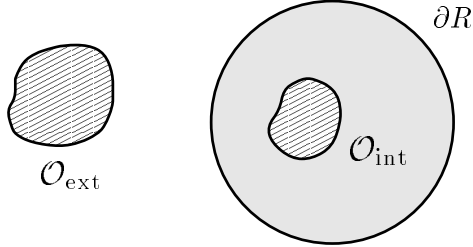


Figure 4: Assumed localization regions of the field products  $\mathcal{O}_{\text{int}}$  and  $\mathcal{O}_{\text{ext}}$  when deriving the integrated Ward identity eq. (17).

the limit where  $\omega^a(x)$  goes to a constant in  $R$ , eq. (14) then becomes

$$\int_{\partial R} d\sigma_\mu(x) \omega^a \langle A_\mu^a(x) \mathcal{O}_{\text{int}} \mathcal{O}_{\text{ext}} \rangle = - \langle \delta \mathcal{O}_{\text{int}} \mathcal{O}_{\text{ext}} \rangle + 2m \int_R d^4x \omega^a \langle P^a(x) \mathcal{O}_{\text{int}} \mathcal{O}_{\text{ext}} \rangle, \quad (17)$$

where the integration on the left-hand side runs over the boundary of  $R$ . So if we set  $m = 0$  and insert  $\mathcal{O}_{\text{int}} = A_\nu^b(y)$ , for example, a little algebra yields

$$\int_{\partial R} d\sigma_\mu(x) \langle A_\mu^a(x) A_\nu^b(y) \mathcal{O}_{\text{ext}} \rangle = i\epsilon^{abc} \langle V_\nu^c(y) \mathcal{O}_{\text{ext}} \rangle \quad (18)$$

with  $V_\nu^c(y)$  being the isovector vector current.

Eq. (18) is reminiscent of the well-known current algebra identities in Minkowski space. Integrating the axial current over the boundary  $\partial R$  effectively amounts to taking the commutator of the axial charge with the fields localized in  $R$ . In particular, the Ward identity eq. (18) simply states that the commutator of the axial charge with the axial current is equal to the vector current. Similar Ward identities may be derived for the isovector vector charge and the whole set of current algebra identities is thus recovered in euclidean space.

#### 4.4 Euclidean proof of the Goldstone theorem

At vanishing quark mass and if chiral symmetry is spontaneously broken through a non-zero value of  $\langle \bar{\psi}\psi \rangle$ , the Goldstone theorem asserts that there exists an isovector of massless bosons (the pions) which couple to the pseudo-scalar density  $P^a(x)$ . In the following lines we give quick proof of this theorem in order to illustrate the power of the chiral Ward identities derived above.

Our starting point is the PCAC relation

$$\langle \partial_\mu A_\mu^a(x) P^a(0) \rangle = 0$$

which holds for all  $x \neq 0$ . Using Lorentz invariance we then deduce that

$$\langle A_\mu^a(x) P^a(0) \rangle = k \frac{x_\mu}{(x^2)^2}$$

for some constant  $k$ . Now if we insert  $\mathcal{O}_{\text{int}} = P^a(0)$  and  $\mathcal{O}_{\text{ext}} = 1$  in the integrated Ward identity eq. (17), and choose  $R$  to be a ball with radius  $r$  centred at the origin, the relation

$$\int_{|x|=r} d\sigma_\mu(x) \langle A_\mu^a(x) P^a(0) \rangle = -\frac{3}{2} \langle \bar{\psi}\psi \rangle$$

is obtained. The constant  $k$  appearing above may thus be calculated and one ends up with

$$\langle A_\mu^a(x) P^a(0) \rangle = -\frac{3}{4\pi^2} \langle \bar{\psi}\psi \rangle \frac{x_\mu}{(x^2)^2}.$$

We can now see that the current-density correlation function is long-ranged if  $\langle \bar{\psi}\psi \rangle$  does not vanish. In particular, the energy spectrum does not have a gap and the correlation function in fact has a particle pole at zero momentum.

#### 4.5 PCAC relation on the lattice

We now pass to the lattice theory and first discuss the PCAC relation. One may be tempted to derive this identity following the steps taken in the continuum theory, but this would not work out because the chiral variation of the lattice action cannot be expressed in terms of the axial current and density alone [31].

We may, however, argue that the position space correlation functions of properly renormalized lattice fields should converge to the corresponding correlation functions in the continuum theory. In particular, if  $(A_R)_\mu^a$  and  $(P_R)^a$  denote the renormalized isovector axial current and density, we expect that

$$\langle \tilde{\partial}_\mu (A_R)_\mu^a(x) \mathcal{O} \rangle = 2m_R \langle (P_R)^a(x) \mathcal{O} \rangle + \mathcal{O}(a) \quad (19)$$

for any product  $\mathcal{O}$  of fields located at non-zero distances from  $x$  (as before the symbol  $\tilde{\partial}_\mu$  stands for the average of the forward and backward difference operators).

The size of the error term in eq. (19) directly tells us how strongly chiral symmetry is violated on the lattice. In particular, in the  $\mathcal{O}(a)$  improved theory the error should be reduced to order  $a^2$  if the coefficients  $c_{\text{sw}}$  and  $c_A$  have their proper values.

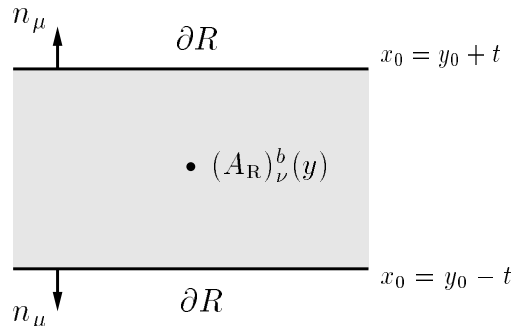


Figure 5: Assumed shape of the region  $R$  in eq. (20). The vector  $n_\mu$  denotes the outward normal to the boundary  $\partial R$ .

This may conversely be taken as a condition to fix these coefficients, a possibility which will be examined in more detail in section 5.

Other applications of the PCAC relation in lattice QCD include the computation of the additive quark mass renormalization  $m_c$  [16] and of the renormalized quark masses (see ref. [45] for a review and an up-to-date list of references).

EXERCISE: Since the flavour symmetry is unbroken on the lattice, there exists an exactly conserved isovector vector current. Deduce the explicit expression for this current

#### 4.6 Chiral symmetry $\mathcal{G}$ renormalization

A well-known theorem states that canonically normalized conserved currents need not be renormalized, because the possible values of the associated charge are fixed algebraically. On the lattice chiral symmetry is violated and the theorem consequently does not apply to the axial current. In general the renormalization constant  $Z_A$  is hence different from 1 and needs to be calculated.

As has been noted a long time ago,  $Z_A$  may be determined through the chiral Ward identities [31,32]. A possible starting point is eq. (18) with  $R$  being the volume between two equal-time hyper-planes (see fig. 5). At zero quark mass and with properly normalized currents we then expect that

$$\begin{aligned}
 a^3 \sum_{x \in \partial R} \epsilon^{abc} n_\mu \langle (A_R)_\mu^a(x) (A_R)_\nu^b(y) \mathcal{O}_{\text{ext}} \rangle \\
 = 2i \langle (V_R)_\nu^c(y) \mathcal{O}_{\text{ext}} \rangle + \mathcal{O}(a)
 \end{aligned}
 \tag{20}$$

for any product  $\mathcal{O}_{\text{ext}}$  of fields localized outside  $R$ . Note that all fields in these correlation functions are in space-time regions well separated from each other. In the  $\mathcal{O}(a)$  improved theory, the error term may hence be expected to be reduced to order  $a^2$ .

Since the left-hand side is proportional to the square of  $Z_A$ , and since the axial current does not appear on the other side of eq. (20), it is quite clear that the renormalization constant can be determined in this way. We shall not go into any further details here, but the idea has been shown to work out in practice and in many cases  $Z_A$  is now known non-perturbatively [33–36].

Once the renormalization constant of the axial current has been determined, the chiral Ward identities may be used to relate the renormalization constants of fields that belong to the same chiral multiplet. The isovector pseudo-scalar density  $(P_R)^a$  and the isoscalar scalar density  $S_R$  transform into each other under chiral rotations and are thus an example of such a multiplet. In this case we would replace  $A_\nu^b(y)$  in eq. (20) by the scalar density. The chirally rotated field then appears on the right-hand side and by evaluating the correlation functions on both sides of the equation one is hence able to fix the relative normalizations of these fields. In principle this procedure generalizes to any chiral multiplet, but some care should be paid when operator mixing occurs.

EXERCISE: On the lattice the local isovector vector current  $V_\mu^a = \bar{\psi}\gamma_\mu\frac{1}{2}\tau^a\psi$  is not exactly conserved. How can one fix the normalization of this current?

#### 4.7 Concluding remarks

Our discussion in this section shows that there are many possibilities to make good use of chiral symmetry in lattice QCD even though the symmetry is not preserved on the lattice. The assumption which has implicitly been made is that the lattice corrections to the chiral Ward identities are small at the accessible lattice spacings. In the unimproved theory this is not obviously the case, because chiral symmetry is violated at order  $a$  and these effects can be rather large as we have previously noted. Further impressive evidence for this will be given below and the bottom-line then is that  $\mathcal{O}(a)$  improvement (or maybe some other form of improvement) should better be applied if one is interested in calculating quantities that are sensitive to chiral symmetry.



## 5 Non-perturbative improvement

As explained in section 3, the coefficients multiplying the various  $O(a)$  counterterms in the improved theory must be tuned to some particular values to achieve the desired improvement. We now show that the coefficient  $c_{\text{sw}}$  appearing in the improved action, eq. (9), can be determined non-perturbatively through the requirement that chiral symmetry is preserved up to terms of order  $a^2$ .

The correlation functions that we shall consider for this purpose are constructed in a finite space-time volume with Dirichlet boundary conditions in the time direction. There are good reasons for this choice, but these will only become clear later. Many technical details will be omitted in the following to keep the basic argumentation transparent. A complete treatment is given in refs. [14–16].

### 5.1 Boundary conditions

The lattices we are going to consider are assumed to have spatial size  $L$  and time-like extent  $T$ , with the time coordinate taking values in the range  $0, a, 2a, \dots, T$ . We impose periodic boundary conditions in all space directions and Dirichlet boundary conditions at time  $x_0 = 0$  and  $x_0 = T$ . The dynamical degrees of freedom of the gauge field are thus the variables  $U(x, \mu)$  associated with the links in the interior of the lattice, while at the boundaries we require that

$$U(x, k)|_{x_0=0} = e^{aC}, \quad U(x, k)|_{x_0=T} = e^{aC'},$$

for all  $k = 1, 2, 3$ . The matrix  $C$  is taken to be constant diagonal,

$$C = \frac{i}{L} \begin{pmatrix} \phi_1 & 0 & 0 \\ 0 & \phi_2 & 0 \\ 0 & 0 & \phi_3 \end{pmatrix}, \quad \phi_1 + \phi_2 + \phi_3 = 0,$$

and  $C'$  is similarly given in terms of another set of angles  $\phi'_\alpha$ .

In the case of the quark field only half of the Dirac components are fixed at the boundaries. The quark propagator is then the solution of a well-posed boundary value problem. Explicitly, if we introduce the projectors  $P_\pm = \frac{1}{2}(1 \pm \gamma_0)$ , the boundary conditions are

$$P_+ \psi(x)|_{x_0=0} = \rho(\mathbf{x}), \quad P_- \psi(x)|_{x_0=T} = \rho'(\mathbf{x}),$$

where  $\rho$  and  $\rho'$  are some externally given (anti-commuting) fields. The corresponding boundary conditions on the anti-quark field are

$$\bar{\psi}(x)P_-|_{x_0=0} = \bar{\rho}(\mathbf{x}), \quad \bar{\psi}(x)P_+|_{x_0=T} = \bar{\rho}'(\mathbf{x}).$$

The field components  $\psi(x)$  and  $\bar{\psi}(x)$  at times  $0 < x_0 < T$  remain unconstrained and represent the dynamical part of the quark and anti-quark fields.

EXERCISE: Consider the free quark theory in the continuum limit with boundary conditions as specified above. Solve the Dirac equation for arbitrary smooth boundary values  $\rho, \rho'$  and prove that the solution is unique

## 5.2 Correlation functions in finite volume

The lattice action in finite volume is essentially given by the expressions that we have written down in the preceding sections for the infinite volume theory. In the case of the  $O(a)$  counterterm in eq. (9), for example, the only modification is that the sum is restricted to all points  $x$  in the interior of the lattice.

Expectation values of products  $\mathcal{O}$  of local fields are now obtained in the usual way through the functional integral. The integration is performed at fixed boundary values, i.e. the integration variables are the unconstrained dynamical field variables residing in the interior of the lattice. In particular, the only dependence on the boundary values  $C, C', \rho, \bar{\rho}, \rho'$  and  $\bar{\rho}'$  arises from the action.

An interesting option at this point is to include derivatives with respect to the quark and anti-quark boundary values in the field product  $\mathcal{O}$ . The operator

$$\mathcal{O}^a = -a^6 \sum_{\mathbf{y}, \mathbf{z}} \frac{\delta}{\delta \rho(\mathbf{y})} \gamma_5 \frac{1}{2} \tau^a \frac{\delta}{\delta \bar{\rho}(\mathbf{z})} \quad (21)$$

is an example of such a product. In the functional integral the derivatives act on the weight factor  $e^{-S}$  and have the effect of inserting certain combinations of the dynamical fields localized near the boundaries of the lattice. More precisely, one finds that in nearly all respects the derivatives  $-\delta/\delta \rho(\mathbf{x})$  and  $\delta/\delta \bar{\rho}(\mathbf{x})$  behave like an anti-quark and a quark field at time  $x_0 = 0$ .

For illustration let us consider the correlation function

$$\langle A_\mu^a(x) \mathcal{O}^a \rangle = \left\{ \frac{1}{\mathcal{Z}} \int_{\text{fields}} A_\mu^a(x) \mathcal{O}^a e^{-S} \right\}_{\rho=\bar{\rho}=\rho'=\bar{\rho}'=0}. \quad (22)$$

Since one sums over the positions  $\mathbf{y}, \mathbf{z}$  in eq. (21), the operator creates a quark and an anti-quark at time zero with vanishing spatial momentum. The correlation function then is proportional to the probability amplitude that the quark anti-quark pair propagates to the interior of the space-time volume and that it annihilates at the point  $x$  (see fig. 6). As usual such pictures have an exact meaning if the quark lines are thought to represent quark propagators at the current gauge field [15].

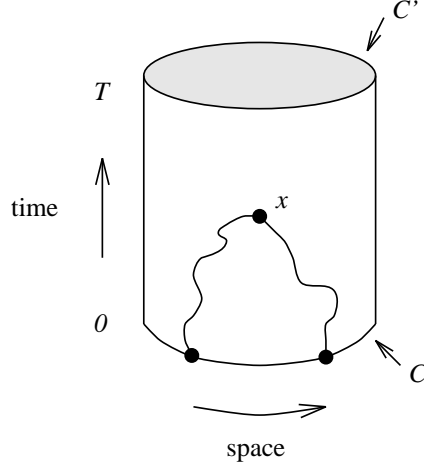


Figure 6: Sketch of the space-time manifold on which the lattice theory is set up.  $C$  and  $C'$  are the boundary values of the gauge field. The irregular lines represent the trajectory of a quark anti-quark pair, which is created at time 0 through the operator  $\mathcal{O}^a$  [eq. (21)].

### 5.3 How large are the chiral symmetry violations?

In principle the error term on the right-hand side of the PCAC relation eq. (19) provides an estimate of the size of chiral symmetry violation in lattice QCD. The renormalization factors in the expressions for the renormalized improved axial current and the associated pseudo-scalar density,

$$\begin{aligned} (A_R)_\mu^a &= Z_A(1 + b_A am_q)\{A_\mu^a + c_A a \tilde{\partial}_\mu P^a\}, \\ (P_R)^a &= Z_P(1 + b_P am_q)P^a, \end{aligned}$$

are however not known at this point and a straightforward calculation of the error term is hence not possible.

Now let us define an unrenormalized current quark mass through

$$m = \frac{\langle \{\tilde{\partial}_\mu A_\mu^a + c_A a \partial_\mu^* \partial_\mu P^a\} \mathcal{O}^a \rangle}{2 \langle P^a \mathcal{O}^a \rangle}, \quad (23)$$

where  $\mathcal{O}^a$  is the operator introduced above. The PCAC relation then implies

$$m = \frac{Z_P(1 + b_P am_q)}{Z_A(1 + b_A am_q)} m_R + \mathcal{O}(a). \quad (24)$$

The renormalization constants and the renormalized mass do not depend on the kinematical parameters such as the time  $x_0$  at which the axial current is inserted or the boundary values  $C$  and  $C'$  of the gauge field. Changing these parameters basically means to probe the PCAC relation in different ways. So if we consider two configurations of the kinematical parameters at the same point  $(g_0, am_0)$  in the bare parameter space, and if  $m_1$  and  $m_2$  denote the associated values of  $m$ , it follows that

$$m_1 - m_2 = O(a). \quad (25)$$

By calculating  $m_1$  and  $m_2$  we thus obtain a direct check on the size of the lattice effects in the PCAC relation.

In the improved theory one expects that the differences in the calculated values of  $m$  are reduced to order  $a^2$ . This may not be totally obvious, because improvement has only been discussed in the context of the infinite volume theory. The boundaries at  $x_0 = 0$  and  $x_0 = T$  indeed require the introduction of further  $O(a)$  counterterms, but since the PCAC relation is locally derived, it can be shown that these affect the relation at order  $a^2$  only [14].

#### 5.4 Tests of chiral symmetry at tree-level of perturbation theory

At vanishing coupling and if  $C = C' = 0$ , the quarks propagate freely and the current quark mass  $m$  is hence expected to coincide with the bare mass  $m_0$  up to lattice effects. A straightforward calculation confirms this and one also finds that  $m$  is independent of the time  $x_0$  at which the axial current is inserted as it should be if lattice effects are negligible.

For non-zero boundary values  $C$  and  $C'$  the situation changes and large lattice effects are observed in the unimproved theory. To illustrate this we consider a  $16 \times 8^3$  lattice and set

$$(\phi_1, \phi_2, \phi_3) = \frac{1}{6} (-\pi, 0, \pi), \quad (\phi'_1, \phi'_2, \phi'_3) = \frac{1}{6} (-5\pi, 2\pi, 3\pi). \quad (26)$$

As shown in fig. 7 the corresponding values of  $m$  strongly deviate from the free quark value and they are also far from being independent of  $x_0$ . These effects almost completely disappear when the improved action is used with  $c_{sw} = 1$  (which is the proper value to this order of perturbation theory). Improvement thus works very well and it is possible to prove that the residual lattice effects seen in fig. 7 are of order  $a^2$  as expected.

The outcome of these calculations can be readily understood if we note that the boundary values  $C$  and  $C'$  induce a background gauge field in the space-time volume, equal to the least action configuration interpolating between  $C$  and  $C'$ .

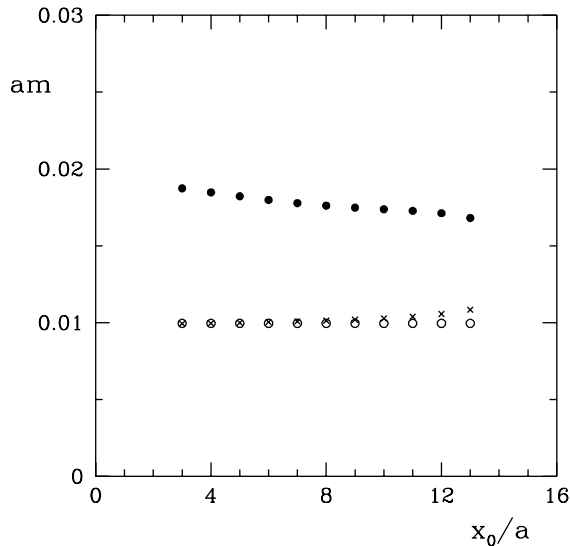


Figure 7: Plot of  $am$  on a  $16 \times 8^3$  lattice with  $am_0 = 0.01$  at tree-level of perturbation theory. The boundary values of the gauge field are zero (open circles) or as given by eq. (26). Full circles and crosses correspond to  $c_{sw} = 0$  and  $c_{sw} = 1$  respectively.

For the boundary values chosen above, the background field can be shown to be a constant colour-electric field given by

$$U(x, \mu) = e^{aB_\mu(x)}, \quad B_0(x) = 0, \quad B_k(x) = C + (C' - C) x_0/T. \quad (27)$$

Now since the lattice effects of order  $a$  can be described by an effective Pauli term, their magnitude is proportional to the strength of the background field and the tests that we have performed are hence directly probing for these effects.

EXERCISE: Check that the PCAC relation is violated by  $O(a^2)$  effects only in the free quark theory on an infinite lattice

### 5.5 Computation of $c_{sw}$

Without improvement the lattice corrections to the PCAC relation are rather large also at the non-perturbative level. This is made evident through fig. 8, where the

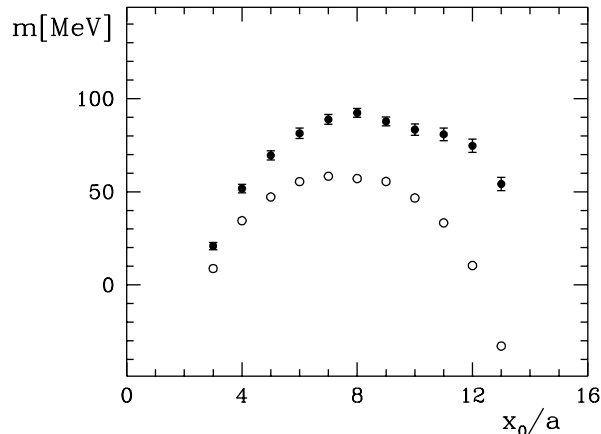


Figure 8: Unrenormalized current quark mass  $m$  on a  $16 \times 8^3$  lattice with spacing  $a = 0.05$  fm, calculated using the unimproved action. Open and full circles correspond to zero and non-zero boundary values of the gauge field.

results of a numerical simulation of the unimproved theory in the quenched approximation are plotted. In this calculation the bare mass  $m_0$  has been set to some value close to  $m_c$  and the bare coupling has been chosen so that  $6/g_0^2 = 6.4$ , which corresponds to a lattice spacing of about 0.05 fm. Again one observes a strong dependence of the calculated values of  $m$  on the background field and also on  $x_0$ .

We may now attempt to adjust the coefficients  $c_{sw}$  and  $c_A$  so as to cancel these effects. This works remarkably well and it is possible to bring almost all points to a well-defined plateau (see fig. 9). Similar results are obtained for larger lattices, other boundary values and so on. In general improvement is very efficient, at least for  $a \leq 0.1$  fm, and with properly chosen  $c_{sw}$  and  $c_A$  the remaining violations of chiral symmetry are small.

### 5.6 Results and further developments

Proceeding in this way the coefficient  $c_{sw}$  has been determined in quenched QCD [16,17] and now also in full QCD with a doublet of dynamical quarks [38]. In the case of full QCD the range of couplings covered extends from small couplings, where contact is made with the one-loop formula eq. (11), up to couplings corresponding to

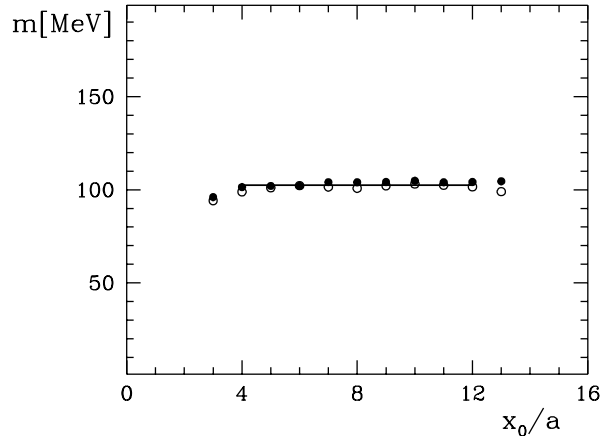


Figure 9: Same as fig. 8, but using the improved action and the improved axial current with  $c_{\text{sw}} = 1.60$  and  $c_A = -0.027$ . The horizontal line is drawn to guide the eye.

$6/g_0^2 \simeq 5.2$ , where the lattice spacing is around 0.1 fm according to some preliminary studies (see fig. 10). The non-perturbative values of  $c_{\text{sw}}$  deviate considerably from the one-loop result at the larger couplings, which is the relevant range for calculations of the hadron masses and other other properties of these particles.

The data shown in fig. 10 are well represented by the rational expression

$$c_{\text{sw}} = \frac{1 - 0.454 g_0^2 - 0.175 g_0^4 + 0.012 g_0^6 + 0.045 g_0^8}{1 - 0.720 g_0^2}. \quad (28)$$

At the level of the numerical accuracy that one has been able to reach, this fit is no worse than the simulation data and it may at this point just as well be taken as the definition of  $c_{\text{sw}}$ . An important remark in this connection is that different ways to calculate  $c_{\text{sw}}$ , using various background fields etc., yield results that differ by terms of order  $a$ . There is nothing fundamentally wrong with this. The systematic uncertainty in  $c_{\text{sw}}$  merely reflects the fact that  $O(a)$  improvement is an asymptotic concept valid up to higher-order terms.

Once  $c_{\text{sw}}$  is known non-perturbatively, one may attempt to calculate the coefficients of other  $O(a)$  correction terms using similar techniques. So far these calculations have been limited to quenched QCD and results have been published for  $c_A$

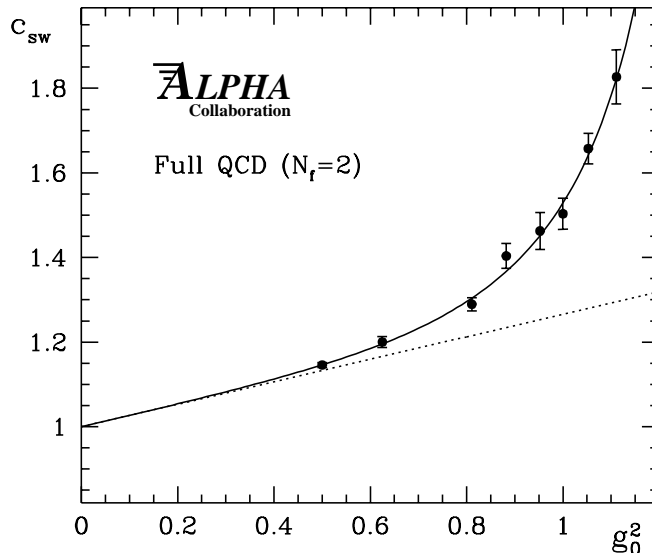


Figure 10: Simulation results for  $c_{sw}$  in QCD with a doublet of dynamical quarks [38]. The solid curve represents the fit eq. (28) and the dotted line the one-loop formula eq. (11).

[16], the  $O(a)$  counterterm needed to improve the isovector vector current [39] and various  $b$ -coefficients [36,20]. Some of these appear to be less accessible and new ideas will be required to be able to compute them [40].

## 6 Non-perturbative renormalization

One of the fundamental problems in QCD is to establish the connection between the low-energy sector and the perturbative regime of the theory. There are many instances where this is required, a particularly obvious case being hadronic matrix elements of operators, whose normalization is specified at high energies through the  $\overline{\text{MS}}$  scheme of dimensional regularization. In the present section we address the issue in the context of lattice QCD and briefly describe some of the techniques that have been proposed to resolve it.



Table 1: Recent results for  $\bar{m}_s$  (quenched QCD,  $\overline{\text{MS}}$  scheme at  $\mu = 2$  GeV)

$\bar{m}_s$ [MeV]	reference
122(20)	Allton et al. (APE collab.) [41]
112(5)	Göckeler et al. (QCDSF collab.) [25]
111(4)	Aoki et al. (CP-PACS collab.) [42]
95(16)	Gough et al. [43]
88(10)	Gupta & Bhattacharya [44]

### 6.1 Example

Let us first discuss one of the standard ways to compute the running quark masses in lattice QCD. The need for non-perturbative renormalization will then become clear. Any details not connected with this particular aspect of the calculation are omitted.

A possible starting point to obtain the sum  $\bar{m}_u + \bar{m}_s$  of the up and the strange quark masses is the PCAC relation

$$m_K^2 f_K = (\bar{m}_u + \bar{m}_s) \langle 0 | \bar{u} \gamma_5 s | K^+ \rangle$$

(lattice effects are ignored here). Since the kaon mass  $m_K$  and the decay constant  $f_K$  are known from experiment, it suffices to evaluate the matrix element on the right-hand side of this equation. On the lattice one first computes the matrix element of the bare operator  $(\bar{u} \gamma_5 s)_{\text{lat}}$  and then multiplies the result with the renormalization factor  $Z_P$  relating  $(\bar{u} \gamma_5 s)_{\text{lat}}$  to the renormalized density  $\bar{u} \gamma_5 s$ .

Some recent results for the strange quark mass obtained in this way or in similar ways are listed in Table 1 (further results can be found in the review of Bhattacharya and Gupta [45]). The sizeable differences among these numbers have many causes. An important uncertainty arises from the fact that, in one form or another, the one-loop formula

$$Z_P = 1 + \frac{g_0^2}{4\pi} \{ (2/\pi) \ln(a\mu) + k \} + O(g_0^4)$$

has been used to compute the renormalization factor, where  $\mu$  denotes the normalization mass in the  $\overline{\text{MS}}$  scheme and  $k$  a calculable constant that depends on the details of the lattice regularization. Bare perturbation theory has long been known to be unreliable at the couplings of interest and without further insight it is clearly impossible to reliably assess the error on the so calculated values of  $Z_P$ . Evidently

this difficulty would go away if we were able to compute the renormalization constant non-perturbatively.

## 6.2 Hadronic renormalization schemes

We now proceed to introduce the notion of a hadronic renormalization scheme and shall then be able to formulate the problem of non-perturbative renormalization in more physical terms.

In a hadronic scheme the renormalization conditions are imposed at low energies by requiring a set of physical quantities, such as the hadron masses and suitable hadronic matrix elements, to assume prescribed values. We may, for example, take the pion decay constant  $f_\pi = 132$  MeV as the basic reference scale and fix the quark masses through the dimensionless ratios

$$m_\pi/f_\pi, m_{K^+}/f_\pi, m_{K^0}/f_\pi, \dots$$

On the lattice the combination  $af_\pi$  then becomes to a function of  $g_0$  alone and a variation in the coupling thus amounts to changing the lattice spacing at constant  $f_\pi$  (and fixed quark masses).

The normalization of local fields can be fixed similarly by requiring the renormalized fields  $\mathcal{O}_R$  to satisfy

$$\langle f | \mathcal{O}_R | i \rangle = \text{prescribed value}$$

for some hadronic states  $|i\rangle$  and  $|f\rangle$ . If there is operator mixing further normalization conditions must be imposed to fix the finite parts of the mixing coefficients.

After these preparations we can now clearly say what non-perturbative renormalization means. Basically what we require is to match a given hadronic scheme with the  $\overline{\text{MS}}$  scheme of dimensional regularization (or any other perturbative scheme). This amounts to calculating the running coupling and quark masses at high energies as well as the renormalization constants  $X_{\mathcal{O}}$  that one needs to convert from the renormalized operators  $\mathcal{O}_R$  to the corresponding fields the  $\overline{\text{MS}}$  scheme.

In principle such a computation is straightforward. The key observation is that all physical amplitudes are uniquely determined functions of the external momenta and the lattice spacing once a definite hadronic scheme has been adopted. We can then consider a set of correlation functions of local fields at large momenta and arrange the momentum cutoff  $\pi/a$  to be far above these scales. Lattice effects are negligible under these conditions and by comparing the exact correlation functions with their perturbation expansion in the  $\overline{\text{MS}}$  scheme one is hence able to extract the running parameters and renormalization constants at normalization scales  $\mu$  given in units of  $f_\pi$  for example.

A subtle technical point here is that the  $\overline{\text{MS}}$  scheme is only defined to every finite order of perturbation theory. The statement that the running coupling etc. can be calculated has, therefore, a precise meaning only in the limit  $\mu/f_\pi \rightarrow \infty$  where higher-order corrections become negligible.

EXERCISE: How precisely are different hadronic schemes related to each other? Convince yourself that it suffices to solve the non-perturbative renormalization problem for one particular hadronic scheme

### 6.3 Meanfield improved perturbation theory

One of the attempts to solve the non-perturbative renormalization problem goes back to an observation of Parisi [46], who noted that the often poor convergence of the bare perturbation expansion may be due to the appearance of so-called tadpole diagrams. Meanfield theory then led him to suggest that these diagrams can be resummed by replacing the coupling  $\alpha_0 = g_0^2/4\pi$  through  $\alpha_P = \alpha_0/P$ , where  $P = 1 - \frac{1}{3}g_0^2 + \dots$  denotes the plaquette expectation value. Manipulations of this sort have later been discussed in greater detail by Lepage and Mackenzie [47] and their recipes are now widely used.

For illustration let us consider the series

$$\alpha_{\overline{\text{MS}}}(\mu) = \alpha_0 + d_1(a\mu)\alpha_0^2 + d_2(a\mu)\alpha_0^3 + \dots, \quad (29)$$

which one obtains by calculating some correlation functions at large momenta using bare perturbation theory and comparing with the expansion in the  $\overline{\text{MS}}$  scheme. For the standard Wilson action the expansion coefficients are known up to two loops [48–50], the result in quenched QCD being

$$\begin{aligned} d_1(a\mu) &= 5.8836 - \frac{11}{2\pi} \ln(a\mu), \\ d_2(a\mu) &= [d_1(a\mu)]^2 + 8.7907 - \frac{51}{4\pi^2} \ln(a\mu). \end{aligned}$$

Note that we do not require  $\mu$  to be much smaller than the momentum cutoff  $\pi/a$ . When deriving the expansion eq. (29), one only needs to know that the external momenta entering the lattice correlation functions that one has chosen to work out are well below this scale. The normalization mass, on the other hand, only appears in the continuum theory and can be arbitrarily large.

To apply these formulae one selects some value of the bare coupling and determines the lattice spacing in the chosen hadronic scheme. This step involves the calculation of meson masses etc. and is hence performed using numerical simulations.

Knowing the lattice spacing in physical units and the bare coupling, the right-hand side of eq. (29) can be evaluated straightforwardly for any given  $\mu$ . On the presently accessible lattices,  $g_0$  is around 1 and  $1/a$  is a few GeV at most. So if we set  $\mu$  to some reasonable value, say 10 GeV, the one- and two-loop terms in the expansion make a contribution roughly equal to 35% and 17% of the leading term. These corrections are not small and there is, therefore, little reason to trust the results that one obtains.

Now if we take Parisi's coupling  $\alpha_P$  as the expansion parameter, the terms in the resulting series tend to be significantly reduced. We may, for example, adjust the scale factor  $a\mu$  so that the one-loop term vanishes and the two-loop correction in the resulting expansion

$$\alpha_{\overline{\text{MS}}}(\mu) = \alpha_P + 2.185 \times \alpha_P^3 + \dots, \quad \mu = 2.633 \times 1/a,$$

then is indeed rather small ( $\alpha_P$  is around 0.13 at the bare couplings of interest). As a consequence one may be more confident in applying this form of the perturbation expansion, although it remains unclear how the truncation error can be estimated in a reliable manner.

#### 6.4 Intermediate renormalization

An interesting method to compute renormalization factors that does not rely on bare perturbation theory has been proposed by Martinelli et al. [51]. The idea is to proceed in two steps, first matching the lattice with an intermediate momentum subtraction (MOM) scheme and then passing to the  $\overline{\text{MS}}$  scheme. The details of the intermediate MOM scheme do not influence the final results and are of only practical importance. One usually chooses the Landau gauge and imposes normalization conditions on the propagators and the vertex functions at some momentum  $p$ . In the case of the pseudo-scalar density, for example, the renormalization constant  $Z_P^{\text{MOM}}$  is defined through

$$\text{Full vertex diagram} = Z_2^{\text{MOM}}/Z_P^{\text{MOM}} \times \text{Bare vertex diagram} \quad (30)$$

where  $Z_2^{\text{MOM}}$  denotes the quark wave function renormalization constant and the diagrams represent the full and the bare vertex function associated with this operator.

On a given lattice and for a range of momenta, the quark propagator and the full vertex function can be computed using numerical simulations [51,52].  $Z_2^{\text{MOM}}$

and  $Z_P^{\text{MOM}}$  are thus obtained non-perturbatively. The total renormalization factor relating the lattice normalizations with the  $\overline{\text{MS}}$  scheme is then given by

$$Z_P(g_0, a\mu) = Z_P^{\text{MOM}}(g_0, ap) X_P^{\text{MOM}}(\bar{g}_{\overline{\text{MS}}}, p/\mu), \quad (31)$$

with  $X_P^{\text{MOM}}$  being the finite renormalization constant required to match the MOM with the  $\overline{\text{MS}}$  scheme.  $X_P^{\text{MOM}}$  is known to one-loop order of renormalized perturbation theory and could easily be worked out to two loops.

While this method avoids the use of bare perturbation theory, it has its own problems, the most important being that the momentum  $p$  should be significantly smaller than  $\pi/a$  to suppress the lattice effects, but not too small as otherwise one may not be confident to apply renormalized perturbation theory to compute  $X_P^{\text{MOM}}$ . It is not totally obvious that these conditions can be met on the currently accessible lattices [53,54] and careful studies should be made to check this.

### 6.5 Recursive finite-size technique

The computational strategies for non-perturbative renormalization discussed so far assume that all relevant physical scales can be accommodated on a single lattice which is sufficiently small for the required calculations to be performed using numerical simulations. As a consequence the energy range where the hadronic scheme can be matched with perturbation theory tends to be rather narrow and it is then not easy to control the systematic errors.

As has been noted some time ago [55], this difficulty can be overcome by simulating a sequence of lattices with decreasing lattice spacings. Any single lattice only covers a limited range of distances, but through the use of a finite-volume renormalization scheme it is possible to match subsequent lattices. Effectively one thus constructs a non-perturbative renormalization group. In a few steps it is then possible to reach much higher energies than would otherwise be possible.

The technique is generally applicable and does not require any uncontrolled approximations to be made [56–59]. Perhaps the greatest difficulty is that the basic strategy does not easily disclose itself. One also needs to perform extensive numerical simulations to set up the non-perturbative renormalization group and there is usually a significant amount of analytical work to be done.

In the following section we discuss the physical picture underlying the technique and introduce some of the key notions. The method itself will then be explained in section 8, taking the computation of the running coupling in quenched QCD as an example.

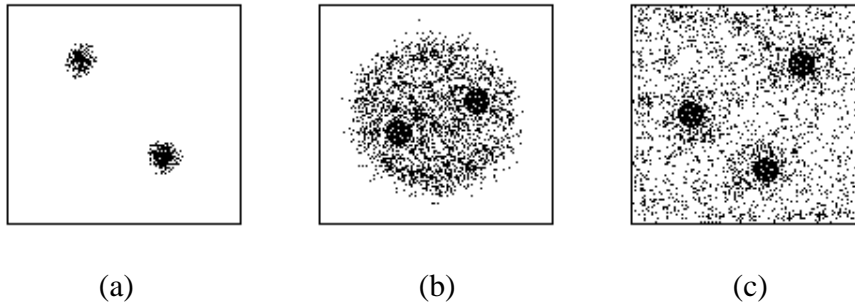


Figure 11: Pictures illustrating various physical situations in finite volume. (a) Hadrons in a large volume, (b) a  $q\bar{q}$  meson in a box of size  $L \simeq 2$  fm, and (c) quarks in the femto-universe.

## 7 QCD in finite volume and the femto-universe

In quantum field theory the physical information is encoded in the correlation functions of local operators and these are hence the primary quantities to consider. From statistical mechanics one knows, however, that certain properties of the system can often be determined more easily by studying its behaviour in finite volume. The calculation of critical exponents is a classical case where such finite-size techniques are being applied.

The questions one would like to answer in QCD are not the same as in statistical mechanics, but the general idea to probe the system through a finite volume proves to be fruitful here too. In this section our aim mainly is to provide a qualitative understanding of what happens when the volume is decreased. Unless stated otherwise, periodic boundary conditions are assumed and the lattice spacing is taken to be much smaller than the relevant physical scales so that lattice effects can be ignored.

### 7.1 Physical situation from large to small volumes

Let us first consider the case where the spatial extent  $L$  of the lattice is significantly greater than the typical size of the hadrons (box (a) in fig. 11). Single hadrons are practically unaffected by the finite volume under these conditions except that their momenta must be integer multiples of  $2\pi/L$ . For multi-particle states the situation is a bit more complicated, because the particles cannot get very far away from each other. Two-particle energy eigenstates, for example, really describe stationary scattering processes. If there are no resonances the corresponding energy values differ from the spectrum calculated for non-interacting particles by small amounts proportional to  $1/L^3$  [60–63].

When  $L$  is 2 fm or so, a single hadron barely fits into the box and the virtual pion cloud around the particle may be slightly distorted (box (b) in fig. 11). In particular, via the periodic boundary conditions it is possible that a pion is exchanged “around the world”. One of the consequences of this effect is that the masses of the hadrons are shifted relative to their infinite volume values by terms of order  $e^{-m_\pi L}$  [60].

At still smaller values of  $L$ , the quark wave functions of the enclosed hadrons are squeezed and one observes rapidly increasing volume effects. Eventually when  $L$  drops below the confinement radius, say  $L \leq 0.5$  fm, the quarks are liberated and hadrons cease to exist (box (c) in fig. 11). QCD in such small volumes is referred to as the femto-universe [64]. Evidently physics is very different in this little world from what one is used to. The chosen boundary conditions play an important rôle, for example, and the energy levels are separated by large gaps that increase proportionally to  $1/L$ .

EXERCISE: Work out the volume dependence of the particle mass in the massive  $\lambda\phi^4$  theory to first order in  $\lambda$ . Check that the volume effects vanish exponentially at large  $L$

## 7.2 Asymptotic freedom and the limit $L \rightarrow 0$

Now if we go to the extreme and allow the box size to become arbitrarily small, we are entering the short distance regime of QCD and thus expect that the effective gauge coupling scales to zero according to the perturbative renormalization group.

To make this a bit more explicit, let us consider the pure gauge theory on a lattice of infinite extent in the time direction and twisted periodic or Dirichlet boundary conditions in the space directions. The reason for this exotic choice is that perturbation theory is much more complicated if periodic boundary conditions are imposed due to the appearance of physical zero modes in the gluon action [65–72]. In this theory an effective gauge coupling may be defined through

$$\alpha_{q\bar{q}} = \left\{ \frac{3}{4} r^2 F_{q\bar{q}}(r, L) \right\}_{r=L/2},$$

where  $F_{q\bar{q}}(r, L)$  denotes the force between static quarks at distance  $r$  in finite volume. Note that  $L$  is the only external physical scale on which this coupling depends.

Perturbation theory at finite  $L$  is more complicated than in infinite volume, but with the chosen boundary conditions no fundamental difficulties are encountered when deriving the Feynman rules. It is possible to set up perturbation theory directly in the continuum theory using dimensional regularization. Alternatively one may choose to work on the lattice and to convert to the  $\overline{\text{MS}}$  scheme later (if so

desired). Proceeding either ways the expansion

$$\alpha_{q\bar{q}} = \alpha_{\overline{\text{MS}}}(\mu) + [(11/2\pi) \ln(\mu L) + k] \alpha_{\overline{\text{MS}}}(\mu)^2 + \dots \quad (32)$$

may be derived and if we set  $\mu = 1/L$  in this equation it is immediately clear that  $\alpha_{q\bar{q}}$  behaves like a running coupling at scale  $L$ .

In full QCD with any number quarks, essentially the same arguments apply and the important conclusion then is that QCD is perturbatively soluble at sufficiently small  $L$ . Eq. (32) also provides a link between the femto-universe and the theory in infinite volume. In particular, if we manage to compute  $\alpha_{q\bar{q}}$  for some box size given in physical units, we could use the relation to determine the  $\overline{\text{MS}}$  coupling at this scale. This may be surprising at first sight, but the equation only reflects the fact that the basic lagrangian is the same independently of the physical context.

### 7.3 Finite-volume renormalization schemes

It should be quite clear at this point that the box size  $L$  may be regarded as a reference scale similar to the normalization mass in the  $\overline{\text{MS}}$  scheme. Renormalization schemes that scale with  $L$  are in fact easily constructed by choosing some particular boundary conditions and by scaling all dimensionful external parameters entering the renormalization conditions with the appropriate power of  $L$ . In particular, if the time-like extent  $T$  of the lattice is finite, the ratio  $T/L$  should be set to some definite value.

The coupling  $\alpha_{q\bar{q}}$  introduced above complies with this general definition and there are many ways to set up finite-volume renormalization conditions for the local operators of interest. The normalization of the isovector pseudo-scalar density, for example, can be fixed through

$$a^6 \sum_{\mathbf{x}, \mathbf{y}} \langle (P_{\text{R}})^a(x) (P_{\text{R}})^a(y) \rangle |_{x_0 - y_0 = L/2} = \text{constant},$$

where the constant should be adjusted so that  $P_{\text{R}}$  has the standard normalization at tree-level of perturbation theory. If zero modes are excluded by the boundary conditions, one can then show that

$$P_{\text{R}} = \{1 + [-(2/\pi) \ln(\mu L) + k] \alpha_{\overline{\text{MS}}}(\mu) + \dots\} P_{\overline{\text{MS}}}(\mu)$$

(with another constant  $k$ ). From the point of view of perturbation theory, finite-volume renormalization schemes are hence as good as any other scheme.

EXERCISE: Invent a finite-volume renormalization condition for the quark masses



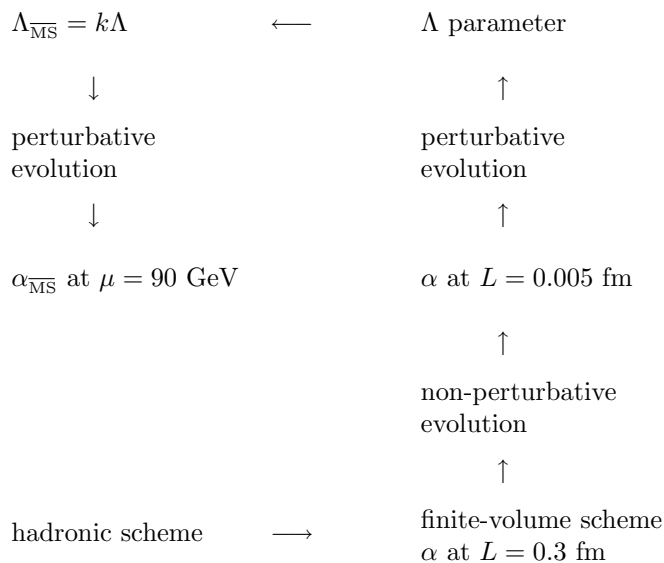


Figure 12: Strategy to compute the running coupling, taking low-energy data as input and using the non-perturbative renormalization group to scale up to high energies.

## 8 Computation of the running coupling

Non-perturbative renormalization is required in many places in lattice QCD, but the calculation of the running coupling is certainly one of the most important cases to consider. As already mentioned in section 6, finite-size techniques allow one to trace the evolution of the coupling from low to high energies and we would now like to describe this in some more detail. Although the method is generally applicable, attention will here be restricted to the pure SU(3) gauge theory. This automatically includes quenched QCD, since the renormalization of the coupling is independent of the valence quarks, but in full QCD a separate calculation will be required.

### 8.1 Strategy

The computation of the running coupling discussed in this section follows the arrows in the diagram shown in fig. 12, starting at the lower-left corner. In this plot the energy is increasing from the bottom to the top while the entries in the left and right columns refer to infinite and finite volume quantities respectively.

In the first step the chosen hadronic scheme is matched at low energies with a suitable finite-volume renormalization scheme. The running coupling in this scheme

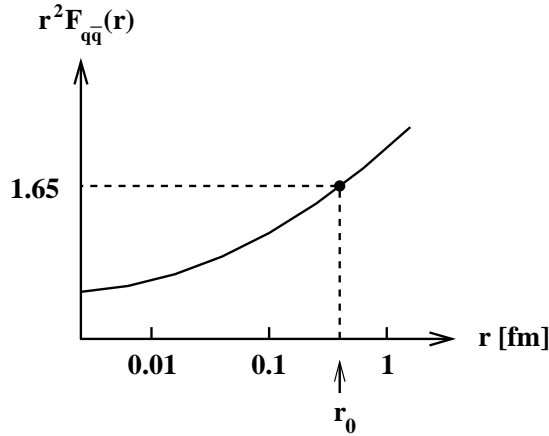


Figure 13: Definition of Sommer's scale  $r_0$ . The dimensionless function  $r^2 F_{q\bar{q}}(r)$  is monotonically rising and  $r_0$  is equal to the distance  $r$  where it passes through 1.65.

is then evolved non-perturbatively to higher energies using a recursive procedure. Eventually the perturbative regime is reached and the  $\Lambda$  parameter can be determined with negligible systematic uncertainty. The conversion to the  $\overline{\text{MS}}$  scheme is trivial at this point (top line of fig. 12).

## 8.2 Hadronic scheme

Since we are considering the pure gauge theory, there are no quark mass parameters to be fixed and a hadronic scheme is defined simply by specifying a low-energy reference scale. We might take the mass of the lightest glueball, for example, but in practice this would not be a good choice, because glueball masses are difficult to compute accurately through numerical simulations.

The force  $F_{q\bar{q}}(r)$  between static quarks at distance  $r$  is more accessible in this respect and may be used to define a reference scale  $r_0$  through [73]

$$r_0^2 F_{q\bar{q}}(r_0) = 1.65 \quad (33)$$

(see fig. 13). Comparing with the phenomenological charmonium potentials, the number on the right-hand side of eq. (33) has been chosen so that  $r_0 \simeq 0.5$  fm. One should however keep in mind that the pure gauge theory is unphysical and an assignment of physical units to  $r_0$  should not be given too much significance.

EXERCISE: At distances  $r \geq 0.3$  fm, the available simulation data for the heavy quark potential are well represented through  $V_{q\bar{q}}(r) = \sigma r - \frac{\pi}{12r} + c$ . Calculate the string tension  $\sigma$  assuming  $r_0 = 0.5$  fm

### 8.3 Finite-volume scheme

We now need to specify the boundary conditions in finite volume and to define a renormalized coupling that scales with  $L$ . For a number of technical reasons, the coupling  $\alpha_{\text{q}\bar{\text{q}}}$  introduced previously is not employed, but in principle this would be an acceptable choice. The definition given below is based on the Schrödinger functional and requires some preparation.

Let us consider a lattice with boundary conditions as specified in section 5 (and no quark fields). Although we have not done so, it is possible to allow for arbitrary space-dependent boundary values and the associated partition function

$$\mathcal{Z}[C', C] = \int_{\text{fields}} e^{-S}$$

is then referred to as the Schrödinger functional. Using the transfer matrix formalism, it is straightforward to show that  $\mathcal{Z}[C', C]$  is equal to the quantum mechanical transition amplitude for going from the field configuration  $C$  at time  $x_0 = 0$  to the configuration  $C'$  at time  $x_0 = T$  [78–84].

At small couplings the functional integral is dominated by the minimal action configuration  $U(x, \mu) = \exp\{aB_\mu(x)\}$  with the specified boundary values. In particular, the perturbation expansion of the Schrödinger functional,

$$\Gamma[B] \equiv -\ln \mathcal{Z}[C', C] = \frac{1}{g_0^2} \Gamma_0[B] + \Gamma_1[B] + g_0^2 \Gamma_2[B] + \dots, \quad (34)$$

is obtained by expanding about this field, which in many respects plays the rôle of a background field. In eq. (34) the leading term is equal to the classical action of the background field, while the higher-order terms require the calculation of Feynman diagrams with propagators and vertices depending on  $B$ .

The renormalizability of the Schrödinger functional has been studied in perturbation theory and it turns out that all ultra-violet divergencies can be cancelled by including the usual counterterms plus a few boundary counterterms in the action [79]. In pure gauge theories boundary counterterms in fact do not occur, because there are no operators with the appropriate dimension and symmetries. The Schrödinger functional is hence a renormalized quantity in this case. In particular, if we choose  $C$  and  $C'$  to depend on some parameter  $\eta$ , it is clear that a renormalized coupling may be defined through [83]

$$\bar{g}^2 = \left\{ \frac{\partial \Gamma_0}{\partial \eta} \bigg/ \frac{\partial \Gamma}{\partial \eta} \right\}_{\eta=0, T=L}. \quad (35)$$

Note that  $L$  is the only external scale in this formula as it should be in a finite-volume renormalization scheme.

The precise choice of the boundary values is largely arbitrary and was made essentially on the basis of practical considerations [56,83]. As in section 5 we take  $C$  and  $C'$  to be constant abelian and set

$$\begin{aligned}(\phi_1, \phi_2, \phi_3) &= \frac{1}{3}(-1, 0, 1)\pi - \frac{1}{2}(-2, 1, 1)\eta, \\(\phi'_1, \phi'_2, \phi'_3) &= \frac{1}{3}(-3, 1, 2)\pi + \frac{1}{2}(-2, 1, 1)\eta.\end{aligned}$$

For small  $\eta$  one can then prove that the background field eq. (27) is the unique absolute minimum of the action [83].

The calculation of  $\bar{g}^2$  through numerical simulations does not present any particular problem. The important point to note is that

$$\partial\Gamma/\partial\eta = \langle\partial S/\partial\eta\rangle$$

is an expectation value of some combination of the gauge field variables close to the boundaries. Since gluon zero modes are excluded through the boundary conditions, the commonly used simulation algorithms remain effective even when  $L$  is very small in physical units.

EXERCISE: Show that the background field eq. (27) solves the lattice field equations. Are there any other gauge inequivalent solutions with the same boundary values?

#### 8.4 Matching at low energies

Returning to the diagram in fig. 12, we first need to match the hadronic scheme with the chosen finite-volume scheme. In the present case this amounts to calculating the coupling  $\bar{g}^2$  at some box size  $L$  given in units of  $r_0$ . Evidently the matching should be done at some convenient point, where both  $r_0$  and  $\bar{g}^2$  can be accurately computed using numerical simulations. Preliminary calculations show that values of  $\bar{g}^2$  around 3.5 are in this range. For definiteness we take

$$L_{\max} \equiv \text{box size where } \bar{g}^2 = 3.480$$

as the matching point and our task then is to determine the ratio  $L_{\max}/r_0$ .

To this end let us choose some value of the bare coupling  $g_0$  where one is able to perform numerical simulations of physically large lattices. Using standard techniques,  $r_0/a$  may then be computed with negligible finite-volume errors [73–77]. At the same coupling one can also simulate lattices with smaller sizes, say  $L/a = 6, 8, \dots, 16$ , and calculate  $\bar{g}^2$  in each case. The renormalized coupling is

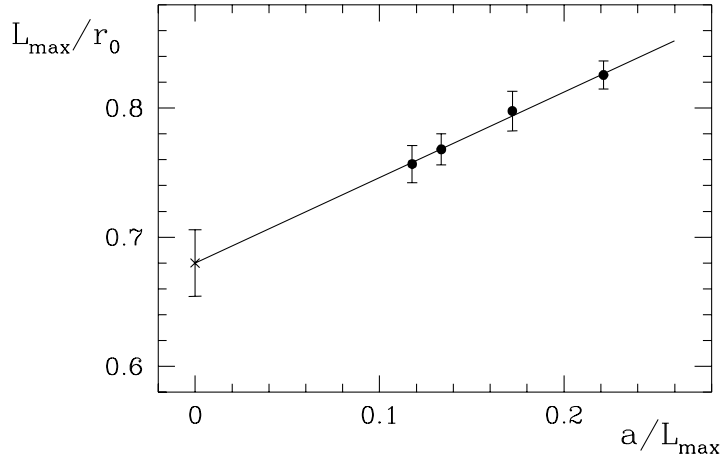


Figure 14: Simulation results for  $L_{\max}/r_0$  and linear extrapolation to the continuum limit (left-most point).

monotonically rising with  $L/a$  and  $L_{\max}/a$  may hence be determined through interpolation to the point where  $\bar{g}^2 = 3.480$  (if it is contained in the range of lattice sizes considered).

Proceeding in this way the ratio

$$L_{\max}/r_0 = (L_{\max}/a)(r_0/a)^{-1}$$

has been calculated at several couplings. Different values of  $g_0$  correspond to different lattice spacings and any variation in the results that obtains thus signals the presence of lattice effects. As shown in fig. 14 the available data decrease linearly with the lattice spacing and after extrapolation to the continuum limit one gets

$$L_{\max}/r_0 = 0.680(26). \quad (36)$$

$L_{\max}$  is thus approximately equal to 0.34 fm in physical units. Note that the observed linear dependence on the lattice spacing is theoretically expected, even though there are no quarks here, because of the presence of the space-time boundaries (see refs. [83,14] for further details).

### 8.5 Non-perturbative renormalization group

We now proceed to scale the renormalized coupling  $\bar{g}^2$  to high energies (small box sizes), taking its value at  $L = L_{\max}$  as initial datum. This will be achieved through

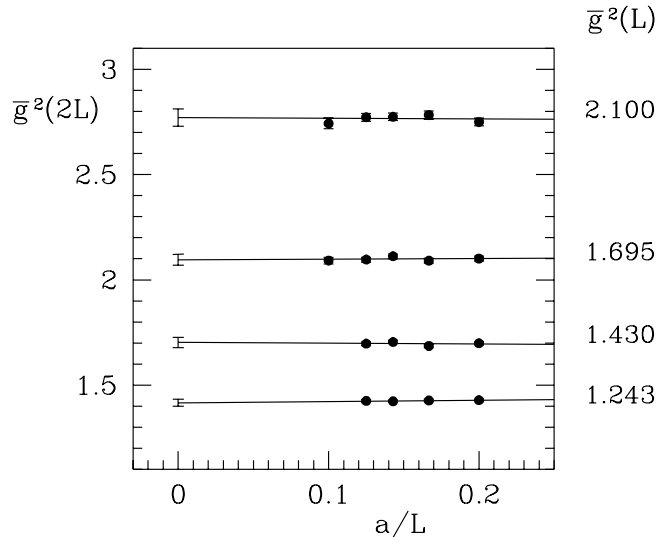


Figure 15: Extrapolation of  $\bar{g}^2(2L)$  to the continuum limit at various values of  $\bar{g}^2(L)$ .

a stepwise procedure in which  $L$  is decreased successively by factors of 2.

Let us first consider the continuum theory, where the scale evolution of the coupling is governed by the renormalization group equation

$$L \frac{\partial \bar{g}}{\partial L} = -\beta(\bar{g}) = b_0 \bar{g}^3 + b_1 \bar{g}^5 + \dots, \quad (37)$$

with  $b_0 = 11(4\pi)^{-2}$  and  $b_1 = 102(4\pi)^{-4}$  being the usual coefficients. This equation determines the coupling at any scale if it is known at some point. In particular, there exists a well-defined function  $\sigma(u)$  such that

$$\bar{g}^2(2L) = \sigma(\bar{g}^2(L)).$$

$\sigma(u)$  may be regarded as an integrated form of the  $\beta$ -function and is referred to as the step scaling function.

The crucial observation now is that  $\sigma(u)$  can be computed on the lattice through numerical simulations. One first chooses some convenient lattice size, say  $L/a = 8$ , and adjusts the bare coupling so that  $\bar{g}^2(L) = u$ . In practice the tuning which is required here does not cause any problems. We may then increase the lattice size by a factor 2 and calculate  $\bar{g}^2(2L)$  at the same value of the bare coupling. The result of this computation is equal to  $\sigma(u)$  up to lattice effects of order  $a$  which can be

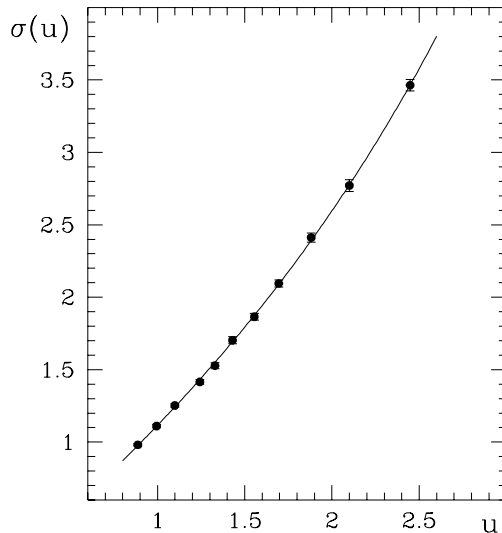


Figure 16: Simulation results for the step scaling function [56,59]. The curve is a polynomial fit with two parameters as described in the text.

extrapolated away by repeating the calculation for several values of  $L/a$ . As shown in fig. 15 the simulation data are in fact independent of the lattice spacing within errors and the continuum limit can thus be easily reached.

Proceeding in this way the step scaling function has been determined for a large range of couplings (see fig. 16). At the smaller couplings the data compare well with the expansion

$$\sigma(u) = u + s_0 u^2 + s_1 u^3 + s_2 u^4 + \dots, \quad (38)$$

which one derives from eq. (37), the first two coefficients being

$$s_0 = 2 \ln(2)b_0, \quad s_1 = 2 \ln(2)b_1 + s_0^2.$$

We may in fact fit all the data by truncating the series at some low order and using the coefficients  $s_2, s_3, \dots$  as fit parameters.

Once the step scaling function is known, the evolution of the coupling can be computed straightforwardly by solving the recursion

$$u_0 = 3.480, \quad u_k = \sigma(u_{k+1}), \quad k = 0, 1, 2, \dots$$

The initial coupling  $u_0$  corresponds  $L = L_{\max}$  and one thus obtains the values of  $\bar{g}^2$  at  $L = 2^{-k} L_{\max}$ . If we demand that  $\sigma(u)$  should only be used in the range of

couplings covered by the data, the recursion can be applied 8 times at most. After six steps, for example, one gets

$$\bar{g}^2 = 1.053(12), \quad L = 2^{-6}L_{\max},$$

where the error has been calculated by propagating the statistical errors to the fit polynomial and solving the recursion using this function. Careful studies have been made to check that this gives correct error bounds and that the results do not depend on the number of fit parameters once a good fit quality is achieved.

EXERCISE: Derive a recursion relation for the coefficients  $s_k$  in eq. (38) assuming the coefficients  $b_k$  of the  $\beta$ -function are known

### 8.6 Computation of the $\Lambda$ parameter

As shown in fig. 17 the data for the coupling  $\alpha = \bar{g}^2/4\pi$  obtained in this way cover a large range of energies from approximately 600 MeV to 150 GeV (using  $L_{\max} = 0.34$  fm to convert to physical units). The perturbative scaling of the coupling sets in rather early and for  $\alpha \leq 0.08$  the data lie on top of the two- and three-loop curves. This may be a bit surprising, but one should not conclude that the absence of large corrections to the perturbative evolution is a general feature of the theory. In other schemes the coupling behaves differently in general and there is usually no way to tell in advance at which energy the non-perturbative contributions become small.

We may now attempt to determine the  $\Lambda$  parameter by scaling the coupling all the way up to infinite energies and taking the limit

$$\Lambda = \lim_{L \rightarrow 0} \frac{1}{L} \lambda(\bar{g}^2), \quad \lambda(u) = (b_0 u)^{-b_1/2b_0^2} e^{-1/2b_0 u}. \quad (39)$$

This is actually not the best way to proceed, because the statistical and systematic errors would not be easy to trace. A better starting point is the exact expression

$$\Lambda = \frac{1}{L} \lambda(\bar{g}^2) \exp \left\{ \frac{1}{2} \int_0^{\bar{g}^2} du \left[ \frac{1}{b(u)} - \frac{1}{b_0 u^2} + \frac{b_1}{b_0^2 u} \right] \right\}, \quad (40)$$

where  $b(u)$  is related to the  $\beta$ -function through

$$b(\bar{g}^2) = -\bar{g}\beta(\bar{g}) = b_0\bar{g}^4 + b_1\bar{g}^6 + \dots$$

Eq. (40) may be proved straightforwardly by noting that the right-hand side is independent of  $L$  and that it has the correct behaviour for  $L \rightarrow 0$ .



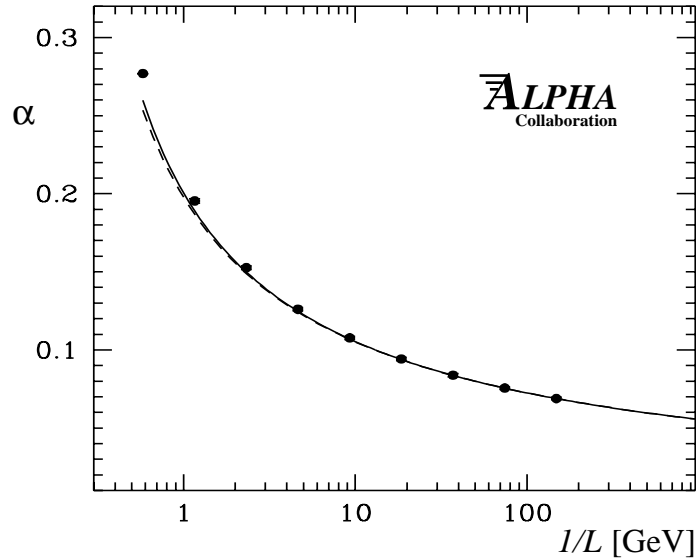


Figure 17: Comparison of simulation results [56,59] for the running coupling (data points) with perturbation theory. The solid (dashed) curve is obtained by integrating eq. (37), starting at the right-most point and using the 3-loop (2-loop)  $\beta$ -function.

To compute the  $\Lambda$  parameter through this formula, one selects some value of  $L$ , say  $L = 2^{-6}L_{\max}$ , where the coupling is known accurately and where it is sufficiently small that the perturbation expansion for the  $b$ -function can be trusted. The series has recently been worked out to three loops [85,86] and using this result to calculate the integral on the right-hand side of eq. (40) one obtains

$$\Lambda = 0.211(16)/L_{\max}. \quad (41)$$

Since the scale evolution of the coupling is accurately reproduced by perturbation theory at high energies, the systematic error arising from the neglected four-loop (and higher-order) corrections to the  $b$ -function are expected to be small. Changing  $L$  from  $2^{-6}L_{\max}$  to  $2^{-8}L_{\max}$  in fact does not have any appreciable effect on the calculated value of the  $\Lambda$  parameter. The influence of a hypothetical four-loop correction can also be estimated by treating this term as a perturbation in eq. (40) and assuming an approximately geometrical progression of the expansion coefficients  $b_k$ . The error bounds that one gets in this way are far below the statistical error and one again concludes that the higher-order contributions can be neglected.

EXERCISE: Estimate the systematic uncertainty on the  $\Lambda$  parameter which would arise if the three-loop coefficient  $b_2$  would not be known

### 8.7 Conversion to the $\overline{\text{MS}}$ scheme

To one-loop order of perturbation theory the relation between the finite-volume and the  $\overline{\text{MS}}$  coupling is given by [56]

$$\alpha = \alpha_{\overline{\text{MS}}}(\mu) + [(11/2\pi) \ln(\mu L) - 1.2556] \alpha_{\overline{\text{MS}}}(\mu)^2 + \dots$$

A short calculation, starting from the definition eq. (39), then leads to the (exact) conversion factor  $\Lambda_{\overline{\text{MS}}}/\Lambda = 2.049$  and if this result is combined with eqs. (36) and (41) one ends up with

$$\Lambda_{\overline{\text{MS}}} = 0.636(54)/r_0. \quad (42)$$

Note that all reference to the intermediate finite-volume scheme has disappeared at this point. Eq. (42) simply expresses the  $\Lambda$  parameter in the  $\overline{\text{MS}}$  scheme in terms of the low-energy scale  $r_0$  and thus provides the solution of the non-perturbative renormalization problem for the running coupling. In physical units, using  $r_0 = 0.5$  fm, one gets  $\Lambda_{\overline{\text{MS}}} = 251(21)$  MeV, but one should not forget that the conversion to physical units is ambiguous in the pure gauge theory. The solid result is eq. (42).

The running coupling  $\alpha_{\overline{\text{MS}}}(\mu)$  at normalization masses  $\mu$  given in units of  $r_0$  may finally be calculated by solving the perturbative renormalization group equation in the  $\overline{\text{MS}}$  scheme, taking eq. (42) as input. The numbers that one obtains tend to be significantly lower than the experimentally measured values of the strong coupling constant, but since we have not included the quark polarization effects there is no reason to be worried. Sea quarks affect the evolution of the coupling (it becomes flatter) and they also influence the low-energy reference scale in some way which is difficult to foresee.

## 9 Conclusions and outlook

One of the greatest advantages of the lattice approach to QCD is that the theory is mathematically well-defined from the beginning. The problem of non-perturbative renormalization, for example, can be given a precise meaning in this framework and its solution then reduces to a mainly computational task. Ultimately the goal is to obtain a clean test of QCD by calculating several quantities with small statistical and systematic errors and comparing the results with experiment. This has not been achieved so far, but the theoretical advances described in these lectures allow one to

be more confident about the basic strategies. In particular, as far as the continuum limit is concerned it now seems unlikely that lattice spacings very much smaller than 0.1 fm will be needed for a reliable computation of the hadron masses and decay constants.

At this point the main problem in lattice QCD is that sea quark effects are not easily included in the numerical simulations. Although the available algorithms have improved over the past few years, the amount of computer time required to simulate even a moderately large lattice is still enormous. As a result of the rapid progress in computer technology, simulations of full QCD are however becoming increasingly feasible. In the meantime the quenched approximation may be used as laboratory to test new ideas and to study more complicated physical problems ( $K \rightarrow \pi\pi$  decays for example).

## References

- [1] K. Symanzik, Cutoff dependence in lattice  $\phi_4^4$  theory, *in*: Recent developments in gauge theories (Cargèse 1979), eds. G. 't Hooft et al. (Plenum, New York, 1980)
- [2] K. Symanzik, Some topics in quantum field theory, *in*: Mathematical problems in theoretical physics, eds. R. Schrader et al., Lecture Notes in Physics, Vol. 153 (Springer, New York, 1982)
- [3] K. Symanzik, Nucl. Phys. B226 (1983) 187 and 205
- [4] K. G. Wilson, Phys. Rev. D10 (1974) 2445
- [5] T. Reisz, Commun. Math. Phys. 116 (1988) 81, 573; *ibid* 117 (1988) 79, 639; Nucl. Phys. B318 (1989) 417
- [6] M. Lüscher, Selected topics in lattice field theory, *in*: Fields, strings and critical phenomena, Les Houches, Session XLIX, eds. E. Brézin and J. Zinn-Justin (Elsevier, Amsterdam, 1990)
- [7] F. Butler et al. (GF11 collab.), Nucl. Phys. B430 (1994) 179
- [8] F. Niedermayer, Nucl. Phys. B (Proc. Suppl.) 53 (1997) 56
- [9] M. Lüscher and P. Weisz, Commun. Math. Phys. 97 (1985) 59 [E: 98 (1985) 433]
- [10] M. Lüscher and P. Weisz, Phys. Lett. 158B (1985) 250
- [11] M. Lüscher, Improved lattice gauge theories, *in*: Critical phenomena, random systems, gauge theories, Les Houches, Session XLIII, eds. K. Osterwalder and R. Stora (Elsevier, Amsterdam, 1986)

- [12] B. Sheikholeslami and R. Wohlert, Nucl. Phys. B259 (1985) 572
- [13] R. Wohlert, Improved continuum limit lattice action for quarks, DESY preprint 87-069 (1987), unpublished
- [14] M. Lüscher, S. Sint, R. Sommer and P. Weisz, Nucl. Phys. B478 (1996) 365
- [15] M. Lüscher and P. Weisz, Nucl. Phys. B479 (1996) 429
- [16] M. Lüscher, S. Sint, R. Sommer, P. Weisz and U. Wolff, Nucl. Phys. B491 (1997) 323
- [17] R. G. Edwards, U. M. Heller and T. R. Klassen, The Schrödinger functional and non-perturbative improvement, hep-lat/9710054
- [18] S. Sint and R. Sommer, Nucl. Phys. B465 (1996) 71
- [19] S. Sint and P. Weisz, Nucl. Phys. B502 (1997) 251
- [20] G. M. de Divitiis and R. Petronzio, Non-perturbative renormalization constants on the lattice from flavor non-singlet Ward identities, hep-lat/9710071
- [21] G. Heatlie, G. Martinelli, C. Pittori, G. C. Rossi and C. T. Sachrajda, Nucl. Phys. B352 (1991) 266
- [22] G. Martinelli, C. T. Sachrajda and A. Vladikas, Nucl. Phys. B358 (1991) 212
- [23] G. Martinelli, C. T. Sachrajda, G. Salina and A. Vladikas, Nucl. Phys. B378 (1992) 591
- [24] C. R. Allton et al. (UKQCD collab.), Phys. Lett. B284 (1992) 377; Nucl. Phys. B407 (1993) 331
- [25] M. Göckeler et al. (QCDSF collab.), Phys. Lett. B391 (1997) 388; Scaling of non-perturbatively  $O(a)$  improved Wilson fermions: hadron spectrum, quark masses and decay constants, hep-lat/9707021
- [26] H. P. Shanahan et al. (UKQCD collab.), Phys. Rev. D55 (1997) 1548
- [27] P. A. Rowland (UKQCD collab.), Improvement and the continuum limit for quenched light hadrons, talk given at the International Symposium on Lattice Field Theory, July 22–26, 1997, Edinburgh; UKQCD collab., in preparation
- [28] A. Cucchieri, M. Masetti, T. Mendes and R. Petronzio, Non-perturbatively improved quenched hadron spectroscopy, hep-lat/9711040
- [29] H. Wittig, Verification of  $O(a)$  improvement, hep-lat/9710013
- [30] R. G. Edwards, U. M. Heller and T. R. Klassen, The effectiveness of non-perturbative  $O(a)$  improvement in lattice QCD, hep-lat/9711052
- [31] M. Bochicchio et al., Nucl. Phys. B262 (1985) 331

- [32] L. Maiani and G. Martinelli, Phys. Lett. B178 (1986) 265
- [33] G. Martinelli, S. Petrarca, C. T. Sachrajda and A. Vladikas, Phys. Lett. B311 (1993) 241 [E: B317 (1993) 660]
- [34] M. L. Paciello, S. Petrarca, B. Taglienti and A. Vladikas, Phys. Lett. B341 (1994) 187
- [35] D. S. Henty, R. D. Kenway, B. J. Pendleton and J.I. Skullerud, Phys. Rev. D51 (1995) 5323
- [36] M. Lüscher, S. Sint, R. Sommer and H. Wittig, Nucl. Phys. B491 (1997) 344
- [37] K. Jansen and C. Liu, Comp. Phys. Commun. 99 (1997) 221
- [38] K. Jansen and R. Sommer, The non-perturbative  $O(a)$  improved action for dynamical Wilson fermions, hep-lat/9709022
- [39] M. Guagnelli and R. Sommer, Non-perturbative  $O(a)$  improvement of the vector current, hep-lat/9709088
- [40] G. Martinelli et al., Phys. Lett. B411 (1997) 141
- [41] C.R. Allton et al. (APE collab.), Nucl. Phys. B431 (1994) 667; *ibid* B489 (1997) 427
- [42] S. Aoki et al. (CP-PACS collab.), CP-PACS result for the quenched light hadron spectrum, hep-lat/9709139
- [43] B. J. Gough et al., Phys. Rev. Lett. 79 (1997) 1622
- [44] R. Gupta and T. Bhattacharya, Phys. Rev. D55 (1997) 7203
- [45] T. Bhattacharya and R. Gupta, Advances in the determination of quark masses, hep-lat/9710095
- [46] G. Parisi, *in*: High-Energy Physics — 1980, XX. Int. Conf., Madison (1980), ed. L. Durand and L. G. Pondrom (American Institute of Physics, New York, 1981)
- [47] G. P. Lepage and P. Mackenzie, Phys. Rev. D48 (1993) 2250
- [48] A. Hasenfratz and P. Hasenfratz, Phys. Lett. B93 (1980) 165; Nucl. Phys. B193 (1981) 210
- [49] M. Lüscher and P. Weisz, Phys. Lett. B349 (1995) 165; Nucl. Phys. B445 (1995) 429; *ibid* B452 (1995) 213, 234
- [50] C. Christou, A. Feo, H. Panagopoulos and E. Vicari, The three-loop  $\beta$ -function of  $SU(N)$  lattice gauge theories with Wilson fermions, hep-lat/9801007
- [51] G. Martinelli et al., Nucl. Phys. B445 (1995) 81

- [52] V. Giménez, L. Giusti, F. Rapuano and M. Talevi, Lattice quark masses: a non-perturbative measure, hep-lat/9801028
- [53] M. Crisafulli et al., Improved renormalization of lattice operators: a critical reappraisal, hep-lat/9707025
- [54] M. Göckeler et al. (QCDSF collab.), Lattice renormalization of quark operators, hep-lat/9710052
- [55] M. Lüscher, P. Weisz and U. Wolff, Nucl. Phys. B359 (1991) 221
- [56] M. Lüscher et al. (ALPHA collab.), Nucl. Phys. B389 (1993) 247; *ibid* B413 (1994) 481
- [57] G. M. de Divitiis et al. (ALPHA collab.), Nucl. Phys. B422 (1994) 382; *ibid* B433 (1995) 390; *ibid* B437 (1995) 447
- [58] K. Jansen et al. (ALPHA collab.), Phys. Lett. B372 (1996) 275
- [59] S. Capitani et al. (ALPHA collab.), Non-perturbative quark mass renormalization, hep-lat/9709125
- [60] M. Lüscher, Commun. Math. Phys. 104 (1986) 177; *ibid* 105 (1986) 153
- [61] M. Lüscher, Nucl. Phys. B354 (1991) 531; *ibid* B364 (1991) 237
- [62] M. Fukugita et al., Phys. Lett. B294 (1992) 380; Phys. Rev. Lett. 73 (1994) 2176; Phys. Rev. D52 (1995) 3003
- [63] S. Aoki et al., Phys. Rev. D50 (1994) 486
- [64] J. D. Bjorken, Elements of quantum chromodynamics, *in*: Proc. Summer Institute on Particle Physics, ed. Anne Mosher, SLAC report no 224 (1980)
- [65] G. 't Hooft, Nucl. Phys. B153 (1979) 141
- [66] M. Lüscher, Phys. Lett. B118 (1982) 391; Nucl. Phys. B219 (1983) 233
- [67] M. Lüscher and G. Münster, Nucl. Phys. B232 (1984) 445
- [68] P. Weisz and V. Ziemann, Nucl. Phys. B284 (1987) 157
- [69] T. H. Hansson, P. van Baal and I. Zahed, Nucl. Phys. B289 (1987) 628
- [70] P. van Baal, Nucl. Phys. B307 (1988) 274 [E: B312 (1989) 752]
- [71] A. Gonzalez-Arroyo and C. P. Korthals-Altes, Nucl. Phys. B311 (1988) 433
- [72] D. Daniel et al., Phys. Lett. B221 (1989) 136; *ibid* B251 (1990) 559
- [73] R. Sommer, Nucl. Phys. B411 (1994) 839
- [74] S. P. Booth et al. (UKQCD collab.), Phys. Lett. B294 (1992) 385
- [75] G. Bali and K. Schilling, Nucl. Phys. B (Proc. Suppl.) 34 (1994) 147

- [76] H. Wittig, Nucl. Phys. B (Proc. Suppl.) 42 (1995) 288; Int. J. Mod. Phys. A12 (1997) 4477
- [77] R. G. Edwards, U. M. Heller and T. R. Klassen, Accurate scale determinations for the Wilson gauge action, hep-lat/9711003
- [78] G. C. Rossi and M. Testa, Nucl. Phys. B163 (1980) 109; *ibid* B176 (1980) 477; *ibid* B237 (1984) 442
- [79] K. Symanzik, Nucl. Phys. B190 [FS3] (1981) 1
- [80] M. Lüscher, Nucl. Phys. B254 (1985) 52
- [81] G. C. Rossi and K. Yoshida, Nuovo Cim. 11D (1989) 101
- [82] J. P. Leroy, J. Micheli, G. C. Rossi and K. Yoshida, Z. Phys. C48 (1990) 653
- [83] M. Lüscher, R. Narayanan, P. Weisz and U. Wolff, Nucl. Phys. B384 (1992) 168
- [84] S. Sint, Nucl. Phys. B421 (1994) 135; *ibid* B451 (1995) 416
- [85] A. Bode, Two-loop expansion of the Schrödinger functional coupling  $\alpha_{\text{SF}}$  in SU(3) lattice gauge theory, hep-lat/9710043
- [86] A. Bode, U. Wolff and P. Weisz, in preparation